Science Co., Saitama, Japan) by the sessile drop method. Drops of purified water (1 μL) were deposited onto the surface modified CLPE with MPC polymer, and the contact angles were directly measured after 60 s by using a microscope according to the ISO 15989 standard.[27] Subsequently, 15 replicate measurements were performed for each sample, and the average values were considered as the contact angles.

Cross-sectional observation by transmission electron microscopy

A cross-section of the PMB30, PMSi90, and PMPC layers on the CLPE surface was observed using a transmission electron microscope (TEM). The specimens were first embedded in epoxy resin, stained with ruthenium oxide vapor at room temperature, and then sliced into ultra-thin films (~100-nm thick) by using a Leica Ultra Cut UC microtome (Leica Microsystems, Wetzlar, Germany). A JEM-1010 electron microscope (JEOL, Tokyo, Japan) was used for the TEM observation at an acceleration voltage of 100 kV.

Characterization of protein adsorption by micro bicinchoninic acid method

The amount of protein adsorbed on the untreated CLPE, PMB30-coated CLPE, PMSi90-coated CLPE, and PMPC-grafted CLPE surfaces was measured by the micro bicinchoninic acid (BCA) method. Each specimen was immersed in Dulbecco's phosphate-buffered saline (PBS, pH 7.4, ion strength = 0.15*M*; Immuno-Biological Laboratories Co., Takasaki, Japan) for 1 h to equilibrate the surface modified by the MPC polymer. The specimens were immersed in bovine serum albumin (BSA, $M_w = 6.7 \times 10^4$; Sigma-Aldrich Corp., MO) solution at 37°C for 1 h. The protein solution was prepared in a BSA concentration of 4.5 g/L, that is, 10% of the concentration of the human plasma levels. Then, the specimens were rinsed five times with fresh PBS and immersed in 1 mass % sodium dodecyl sulfate (SDS) aqueous solution, and shaken at room temperature for 1 h to completely detach the adsorbed BSA on the surface modified by the MPC polymer. A protein analysis kit (micro BCA protein assay kit, No. 23235; Thermo Fisher Scientific, IL) based on the BCA method was used to determine the BSA concentration in the SDS solution, and the amount of BSA adsorbed on the surface modified by the MPC polymer was calculated.

Friction test

A friction test was performed using a ball-on-plate machine (Tribostation 32; Shinto Scientific Co., Tokyo, Japan). Each of the untreated CLPE, PMB30-coated CLPE, PMSi90-coated CLPE, and PMPC-grafted CLPE surfaces was used to prepare six sample pieces. A Co-Cr-Mo alloy ball with a diameter of 9 mm was prepared. The surface roughness of the ball was Ra $\geq$ 0.01, which was comparable to that of femoral ball products. The friction tests were performed at room temperature with various loads in the range of 0.49–9.80 N, sliding distance of 25 mm, and frequency of 1 Hz for a maximum of 100 cycles.[28] Pure water was used as a lubricant medium. The mean coefficients of dynamic friction were determined by averaging five data points from the 100 (96–100) cycle measurements.

Hip joint simulator wear test

A 12-station hip joint simulator (MTS Systems Corp., MN) with the untreated CLPE, PMB30-coated CLPE, PMSi90-coated CLPE, and PMPC-grafted CLPE cups (n = 2), both having inner and outer diameters of 26 and 52 mm, respectively, was used for the hip joint simulator wear test. A Co-Cr-Mo alloy femoral ball component with a size of 26 mm (Japan Medical Materials Corp., Osaka, Japan) was used as the femoral component. A mixture of 25 vol % bovine serum, 20 m*M*/L of ethylene diamine tetraacetic acid, and 0.1 mass % sodium azide was used as a lubricant, according to the ISO 14242-1 standard.[29] The lubricant was replaced every 0.5×10^6 cycles. Walks that simulated a physiologic loading curve (Paul-type), with double peaks at 1793 and 2744 N loads with a multidirectional (biaxial and orbital) motion of 1 Hz frequency, were applied. The wear was determined by weighing the cups at intervals of 0.5×10^6 cycles. Load-soak controls (n = 2) were used to compensate the fluid absorption by the specimens.[30] The testing was continued until a total of 3.0×10^6 cycles were completed.

Statistical analysis

The results derived from each measurement in the water-contact angle estimation, friction test, and protein adsorption test were expressed as mean values and standard deviation. The statistical significance ($p < 0.05$) was estimated by Student's t-test.

RESULTS

Figure 2 shows the FTIR/ATR spectra of the untreated CLPE, PMB30-coated CLPE, PMSi90-coated CLPE, and PMPC-grafted CLPE. An absorption peak was observed at 1460 cm^{-1} for all test specimens. This peak is mainly attributed to the methylene (CH_2) chain in the CLPE substrate and the MPC polymer chain. However, absorption peaks at 1240, 1080, and 970 cm^{-1} were observed only for the CLPE, whose surface was modified by the MPC polymer. These peaks corresponded to the phosphate group (P—O) in the MPC unit. Similarly, an absorption peak at 1720 cm^{-1} observed in the surface modified CLPE corresponded only to the carbonyl group (C=O) in the MPC unit. The absorption peak intensity of the P—O group of the PMPC-grafted CLPE was the highest in the CLPE, whose surface was modified by the MPC polymer.

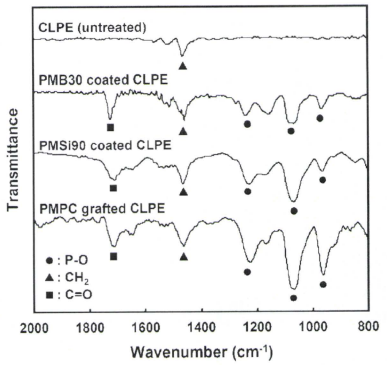

Figure 2. FTIR/ATR spectra of untreated CLPE, MPC polymer-coated CLPE, and PMPC-grafted CLPE.

Table I summarizes the surface elemental compositions of the untreated CLPE, PMB30-coated CLPE, PMSi90-coated CLPE, and PMPC-grafted CLPE. The nitrogen (N) and phosphorous (P) contents in all the CLPE specimens, whose surface were modified by the MPC polymer, were observed. The surface elemental compositions of both N and P in the surface modified CLPE increased with an increase in the MPC composition in the polymer for surface modification. In particular, the elemental compositions of N and P in the PMPC-grafted CLPE surface were 5.2 and 5.3 atom %, respectively. The elemental composition of the PMPC-grafted CLPE surface was almost equivalent to the theoretical elemental composition ($N = 5.3$, $P = 5.3$ atom %) of PMPC.

Figure 3 shows the cross-sectional TEM images of the untreated CLPE, PMB30-coated CLPE, PMSi90-coated CLPE, and PMPC-grafted CLPE. For the PMB30 and PMSi90 coatings, and PMPC grafting, a 100-nm thick MPC polymer layer was clearly observed on the surface of the CLPE substrate. No crack for poor adhesion and/or delamination was observed at the interface between MPC polymer layer and CLPE substrate. These results indicate that each surface modification layer on the CLPE substrate is uniform and cover closely, regardless of the binding conditions: the surface modification layers by the PMB30 and PMSi90 coatings, and PMPC grafting are combined with the substrate by physical adsorption and covalent bonds of Si—O—C and C—C, respectively. In the PMB30-coated CLPE, a bilayer structure attributed to dipping twice was clearly observed on the surface modification layer.

Figure 4 shows the static water-contact angles of the untreated CLPE, PMB30-coated CLPE, PMSi90-coated CLPE, and PMPC-grafted CLPE. The static water-contact angles of the untreated CLPE and PMB30-coated CLPE were 90° and 100°, respectively, and they decreased markedly to ~10° (i.e., 8°–13°, $p < 0.001$) by the PMSi90 coating and PMPC grafting.

Figure 5 shows the amount of BSA adsorbed on the surfaces of the untreated CLPE, PMB30-coated CLPE, PMSi90-coated CLPE, and PMPC-grafted CLPE. The amount of BSA adsorbed on the CLPE surface modified by the MPC polymer was considerably lesser ($p < 0.001$) than that of the untreated CLPE, that is, 0.05–0.10 μg/cm^2. These results imply that the surface modification by the MPC polymer results in good biocompatibility.

Figure 6 shows the coefficients of dynamic friction of the untreated CLPE, PMB30-coated CLPE, PMSi90-coated CLPE, and PMPC-grafted CLPE. As compared to the untreated specimens, the PMB30-coated and PMSi90-coated CLPE specimens showed a reduction of ~30% (i.e., 25–30%, not significant) in their coefficients of dynamic friction. Further, as compared to the untreated CLPE specimens, the PMPC-grafted CLPE specimens showed a reduction of ~84% ($p < 0.005$) in their coefficients of dynamic friction.

Figure 7 shows the coefficients of dynamic friction of the untreated CLPE, PMB30-coated CLPE, PMSi90-coated CLPE, and PMPC-grafted CLPE as a function of the loads in the ball-on-plate friction test. The untreated CLPE showed the highest coefficient of dynamic friction, that is, ~0.075. This value was almost constant throughout the experiment. The coefficients of dynamic friction of the PMB30-coated

TABLE I
Surface Elemental Composition (atom %) of CLPE, MPC Polymer Coated CLPE, and PMPC Grafted CLPE ($n = 5$)

Sample	C	O	N	P	Si
CLPE (untreated)	99.8 (0.3)[a]	0.2 (0.3)	0.0 (0.0)	0.0 (0.0)	0.0 (0.0)
PMB30 coated CLPE	69.9 (1.0)	25.5 (0.6)	2.1 (0.2)	2.5 (0.3)	0.0 (0.0)
PMSi90 coated CLPE	60.5 (0.7)	30.4 (0.4)	4.1 (0.2)	4.0 (0.2)	1.0 (0.0)
PMPC grafted CLPE	58.0 (0.2)	31.5 (0.2)	5.2 (0.1)	5.3 (0.1)	0.0 (0.0)
PMPC[b]	57.9	31.6	5.3	5.3	0.0

[a]The standard deviation is in parentheses.
[b]Theoretical elemental composition of PMPC.

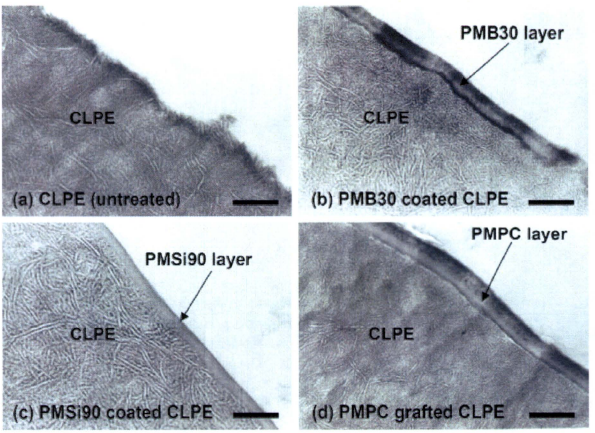

Figure 3. Cross-sectional TEM images of untreated CLPE, MPC polymer-coated CLPE, and PMPC-grafted CLPE. Bar: 200 nm.

CLPE and PMSi90-coated CLPE were smaller (~0.055) than those of the untreated CLPE at loads of up to 0.98 N; then, these coefficients increased to the level of the coefficients of the untreated CLPE at loads above 1.96 N. For both PMB30-coated CLPE and PMSi90-coated CLPE, the MPC polymer layer coating showed almost the same coefficients of dynamic friction. The PMPC-grafted CLPE showed a remarkably low friction coefficient of ~0.026 at a load of 0.49 N; this value decreased gradually and reached ~0.005 at a load of 9.80 N.

Figure 8 shows the gravimetric wear of the untreated CLPE, PMB30-coated CLPE and PMSi90-coated CLPE, and PMPC-grafted CLPE cups in the hip simulator wear test. It was observed that the wear in the PMPC-grafted CLPE cups was significantly lower than that in the untreated CLPE cups. There was no significant difference in the wear of the untreated CLPE and PMB30-coated CLPE cups. The PMSi90-coated CLPE cups showed slightly lower wear than the untreated CLPE cups; however, the weight change varied for each cup (standard

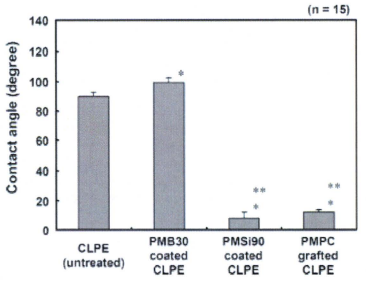

Figure 4. Static-water contact angle of untreated CLPE, MPC polymer-coated CLPE, and PMPC-grafted CLPE. Bar: Standard deviations. *: Significant difference ($p < 0.001$) as compared to the untreated CLPE, **: significant difference ($p < 0.001$) as compared to the PMB30-coated CLPE.

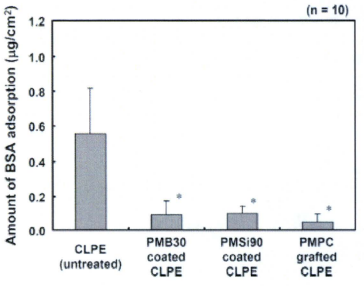

Figure 5. Amount of BSA adsorbed on the surfaces of the untreated CLPE, MPC polymer-coated CLPE, and PMPC-grafted CLPE. Bar: Standard deviations. *: Significant difference ($p < 0.001$) as compared to the untreated CLPE.

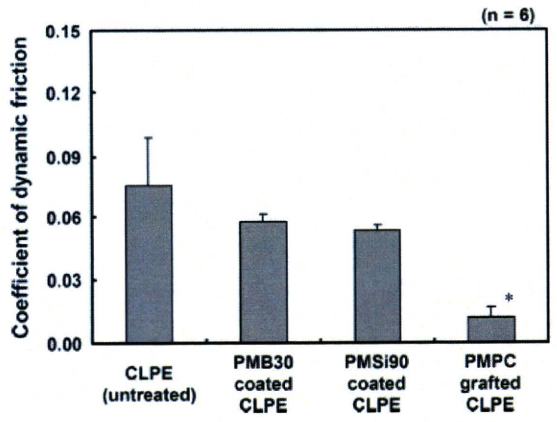

Figure 6. Coefficients of dynamic friction of untreated CLPE, MPC polymer-coated CLPE, and PMPC-grafted CLPE. Bar: Standard deviations. *: Significant difference ($p < 0.005$) as compared to the untreated CLPE.

deviation = ±9.0 mg). The PMPC-grafted CLPE cups showed a slight increase in weight. This was partially attributable to the enhanced fluid absorption in the tested cups as compared to that in the load-soak controls. While applying the gravimetric method, the weight loss in the tested cups is corrected by subtracting the weight gain in the load-soak controls; however, this correction cannot be achieved perfectly because only the tested cups are continuously subjected to motion and load. Usually, the fluid absorption in the tested cups is generally slightly higher than that in the load-soak controls. Consequently, the correction of the fluid absorption by using the load-soak data as the correction factor leads to a slight underestimation of the actual weight loss.[22,29] In this study, a steady wear rate was calculated using data from 2.0×10^6 to 3.0×10^6 cycles; in the untreated CLPE, PMB30-coated CLPE, and PMSi90-coated CLPE cups, these rates were 6.1, 5.9, and 4.5 mg/10^6 cycles, respectively. In contrast, the wear rate of the PMPC-grafted CLPE cups was markedly lower, that is, −1.5 mg/10^6 cycles.

DISCUSSION

In this study, we have investigated the surface properties of various surface modification layers formed on the CLPE surface by the physical and chemical coating of the MPC polymers or photoinduced radical grafting of MPC. Here, we discuss the durability of the CLPE whose surface is modified by the MPC polymer in terms of the characteristics of the nanometer-scale layer of the MPC polymer.

The layer, whose surface contains the physically coated PMB30, is combined with the substrate by physical adsorption.[11,12] The layer, whose surface contains the chemically coated PMSi90, is combined with the substrate by physical adsorption and/or slight Si—O—C covalent bonding ascribed to the 10% MPSi in the PMSi90 composition; a hydrolyzed silane molecule of PMSi90 has three —OH groups that react with the —OH groups of the surface oxide layer of the CLPE substrate induced by the O_2 plasma irradiation, and they form covalently siloxane bonds.[27] On the other hand, the surface modification layer obtained by PMPC grafting is combined with the substrate by strong C—C covalent bonding.[19–24]

In Figure 7, the coefficients of dynamic friction of the PMB30-coated CLPE and PMSi90-coated CLPE increased to the level of the coefficient of dynamic

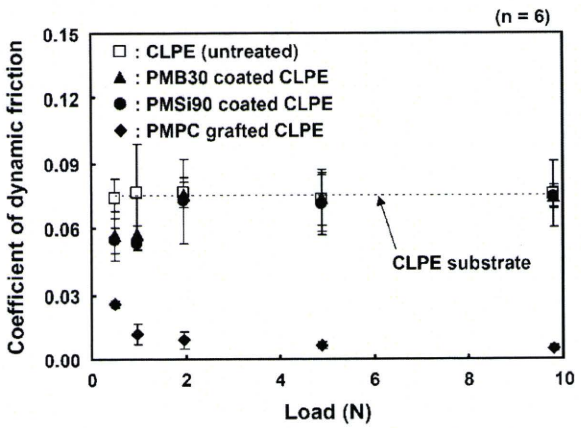

Figure 7. Coefficients of dynamic friction of the untreated CLPE, MPC polymer-coated CLPE, and PMPC-grafted CLPE as a function of loads in the ball-on-plate friction test. Bar: Standard deviations.

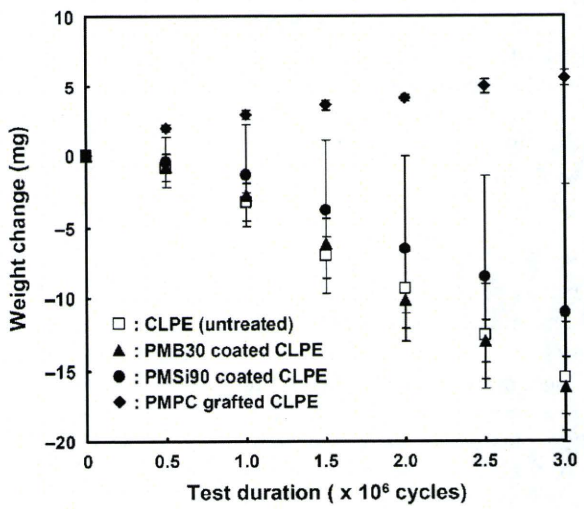

Figure 8. Weight change (volumetric wear) of the untreated CLPE, MPC polymer-coated CLPE, and PMPC-grafted CLPE in the hip joint simulator wear test. Bar: Standard deviations.

friction of the untreated CLPE at loads above 1.96 N. In addition, as shown in Figure 8, there was no significant difference in the wear of the untreated CLPE and the MPC polymer coated CLPE cups in the hip joint simulator tests. In contrast, the PMPC-grafted CLPE showed an extremely low and stable coefficient of dynamic friction and volumetric wear as compared to the untreated CLPE and MPC polymer coated CLPE, as shown in Figures 7 and 8. These results indicate that the PMB30 and PMSi90 surface modification layers are removed from the CLPE surface. The surface modification layers by the PMB30 and PMSi90 coatings are combined with the substrate by physical adsorption and chemical bonds of Si—O—C, respectively. Therefore, the physical adsorption and chemical bonds of Si—O—C are ineffective in the case of large and multidirectional loads. The chemical bonds of Si—O—C are probably insufficient, because the MPSi composition in the PMSi90 polymer is 10%. Therefore, it is thought that a sufficient number of strong bonds between the surface modification layer and the CLPE surface are essential for the long-term retention of the benefits of the MPC polymer used in artificial joints under variable and multidirectional loads.

Since MPC is a highly hydrophilic compound, the MPC polymers PMSi90 and PMPC are water-soluble. The water-wettability of the PMSi90-coated and PMPC-grafted CLPE surfaces with a high MPC unit mole fraction (90 and 100%) was considerably greater than that of the untreated CLPE surface, as shown in Figure 4. Kobayashi et al. reported that the water molecules adsorbed on the surface of the highly hydrophilic PMPC act as lubricants and reduce the interaction between the PMPC and the counter-bearing face.[31] Therefore, it is thought that the artificial hip joint bearing with the PMSi90-coated and PMPC-grafted surfaces exhibited considerably higher lubricity than that with the untreated CLPE. The amount of water molecules absorbed on the surface of the CLPE (water thin-film) is expected to play an important role with regard to the property of low friction.

However, in reality fact as shown in Figure 6, the PMSi90-coated CLPE specimens exhibited a maximum reduction of ~30% in their coefficients of dynamic friction as compared to the untreated CLPE specimens. In contrast, the PMPC-grafted CLPE specimens exhibited a reduction of ~84%. It was previously reported that the polymer concentration (i.e., viscosity) increased with the friction coefficient in the mixed lubrication regime.[32] Therefore, It is assumed that an ultra-low friction of PMPC-grafted CLPE that occurs during sliding is related to the effective viscosity of the PMPC in the mixed lubrication of the intermediate hydrated layer. The high-density PMPC graft chains in the PMPC-grafted CLPE are assumed to exhibit a brush-like structure.[25,33] The viscosity of the PMPC layer reflects the mobility of the free end groups of the MPC polymer or MPC polymer chains themselves.[34,35] In contrast, the mobility of PMSi 90 is limited by the cross-linking and network entanglement of the gel structure of PMSi90. Hence, we think that the polymer brush-like structure of the PMPC-grafted CLPE with high mobility of polymer chains can function as a considerably better surface hydration lubrication system of artificial joints than the gel structure of the PMSi90-coated CLPE. These considerations are based on the previous studies on charged polymers (polyelectrolytes) by Klein and coworkers.[34,35]

The significant reduction in the coefficient of friction of the grafted PMPC resulted in a substantial improvement in wear resistance. A previous study reported that the hydrogel cartilage surface was assumed to have a brush-like structure: a part of the proteoglycan aggregate brush bonds with the collagen network in the cartilage surface.[36] It is thought that the bearing surface with high-density PMPC in artificial hip joints has a brush-like structure similar to an articular cartilage. We assume that the bearing surface of the artificial hip joint combined with a 100-nm thick MPC polymer layer results in a fluid film lubrication (or mixed lubrication) of the intermediate hydrated layer; which suggests that this novel artificial hip joint mimics the natural joint cartilage.

As shown in Figure 7, the coefficients of dynamic friction of the untreated CLPE surface were constant for all load values. In contrast, those of the PMPC-grafted CLPE surface decreased with increasing load. These results show that the PMPC-grafted layer does not follow Amonton's law of $F = \mu N$. The maximum contact stress of ~62 MPa at a load of 9.8 N is higher than the yield tensile strength of the CLPE (~23 MPa). The maximum contact stress is roughly calculated by the Hertzian theory. The elastic CLPE substrate is deformed slightly by the loads, the low friction coefficient may have been shown in order to get much more amount of water thin-film with the larger contact area of concave surface. We also think that these results imply that the lubrication of the PMPC-grafted CLPE is dominated by the hydrodynamic lubrication mechanism.

As shown in Figure 4, the static water-contact angle of the PMB30-coated CLPE was ~100°. Sibarani et al. reported that the PMB30-coated polymer surfaces showed high advancing (~100°) and low receding (~20°) contact angles.[5] Moreover, Yamasaki et al. reported that the PMB30-coated polymer surfaces required more than 30–300 min to achieve complete equilibrium.[37] This indicates that the PMB30 cannot be hydrated easily, due to the low MPC unit composition of the copolymer and low mobility of

the polymer chain. However, as shown in Figure 5, the PMB30-coated CLPE surface, which could form a phosphorylcholine-enriched surface after equilibrating for 1 h, showed excellent biocompatibility as an antiadsorption surface for BSA.

The adsorption of the representative plasma protein, BSA, on the CLPE surface decreased to 9–18% due to the surface modification by the MPC polymer, as shown in Figure 5. It is hypothesized that the mechanism of protein adsorption resistivity on the surface modified by the MPC polymer is based on the water structure resulting from the interactions between water molecules and phosphorylcholine groups.[26,37,38] The large amount of free water around the phosphorylcholine group is considered to detach proteins easily and even prevent conformational changes in the adsorbed proteins.[26,38] Hence, we expect that the protein adsorption will decrease with increasing MPC unit composition in the MPC copolymer. However, in this study, there was no significant difference in the protein adsorption of the CLPE, whose surfaces was modified by the MPC polymer (the MPC unit compositions were 30, 90, and 100%). The reduction in protein adsorption is also considered to be caused by the presence of a hydrated layer around the phosphorylcholine group.[26,39] The latter consideration is consistent with the results of the water contact angle measurement, friction test, and cross-sectional TEM observations of the CLPE, whose surface is modified CLPE by the MPC polymer (Figs. 3, 4, and 6). The previous studies reported that the protein concentration of lubricants such as bovine serum considerably affected the wear rate of the UHMWPE cups in the joint simulator test: the protein concentrations in the synovial fluids of both normal and diseased joints (~20–40 mg/mL), including joints after total arthroplasty, were associated with the highest wear rates.[40,41] We think that the antiprotein adsorption surface on the CLPE prepared by the MPC polymer will prevent the highest adhesive wear rates *in vivo* caused by the protein adsorption. Moreover, the CLPE whose surface is modified by the MPC polymer is expected to exhibit tissue and blood compatibility as biocompatibility, because previous studies have reported that the MPC polymer modified surfaces exhibit *in vivo* biocompatibility.[3–11]

CONCLUSION

In this study, we systematically investigated the surface properties of the various surface modification layers formed on the CLPE surface by the MPC polymer by dip coating or photoinduced radical grafting. It is concluded that several important issues are involved in the long-term retention of the benefits of the MPC polymer used in artificial joints under variable and multidirectional loads, for example, strong bonding between the MPC polymer and the CLPE surface and high mobility of the free end groups of the MPC polymer. We should employ the photoinduced radical graft polymerization to create strong covalent bonding between the CLPE substrate and the surface modification layer, and also to retain the high mobility of polymer chains of that layer.

The authors express special thanks to Dr. Masaru Ueno (Japan Medical Materials Corp.), and Dr. Kikuko Fukumoto, Ms. Emi Tabata, and Ms. Satomi Shinbashi (The University of Tokyo) for their excellent technical assistance.

References

1. Iwasaki Y, Ishihara K. Phosphorylcholine-containing polymers for biomedical applications. Anal Bioanal Chem 2005; 381:534–546.
2. Binyamin G, Shafi BM, Mery CM. Biomaterials: A primer for surgeons. Semin Pediatr Surg 2006;15:276–283.
3. Ishihara K, Iwasaki Y, Ebihara S, Shindo Y, Nakabayashi N. Photoinduced graft polymerization of 2-methacryloyloxyethyl phosphorylcholine on polyethylene membrane surface for obtaining blood cell adhesion resistance. Colloids Surf B Biointerfaces 2000;18:325–335.
4. Kyomoto M, Iwasaki Y, Moro T, Konno T, Miyaji F, Kawaguchi H, Takatori Y, Nakamura K, Ishihara K. High lubricious surface of cobalt-chromium-molybdenum alloy prepared by grafting poly(2-methacryloyloxyethyl phosphorylcholine). Biomaterials 2007;28:3121–3130.
5. Sibarani J, Takai M, Ishihara K. Surface modification on microfluidic devices with 2-methacryloyloxyethyl phosphorylcholine polymers for reducing unfavorable protein adsorption. Colloids Surf B Biointerfaces 2007;54:88–93.
6. Ueda T, Oshida H, Kurita K, Ishihara K, Nakabayashi N. Preparation of 2-methacryloyloxyethyl phosphorylcholine copolymers with alkyl methacrylates and their blood compatibility. Polym J 1992;24:1259–1269.
7. Konno T, Ishihara K. Temporal and spatially controllable cell encapsulation using a water-soluble phospholipid polymer with phenylboronic acid moiety. Biomaterials 2007;28:1770–1777.
8. Xu Y, Takai M, Konno T, Ishihara K. Microfluidic flow control on charged phospholipid polymer interface. Lab Chip 2007;7:199–206.
9. Snyder TA, Tsukui H, Kihara S, Akimoto T, Litwak KN, Kameneva MV, Yamazaki K, Wagner WR. Preclinical biocompatibility assessment of the EVAHEART ventricular assist device: Coating comparison and platelet activation. J Biomed Mater Res A 2007;81:85–92.
10. Ueda H, Watanabe J, Konno T, Takai M, Saito A, Ishihara K. Asymmetrically functional surface properties on biocompatible phospholipid polymer membrane for bioartificial kidney. J Biomed Mater Res A 2006;77:19–27.
11. Kuiper KK, Nordrehaug JE. Early mobilization after protamine reversal of heparin following implantation of phosphorylcholine-coated stents in totally occluded coronary arteries. Am J Cardiol 2000;85:698–702.
12. Ishihara K, Ueda T, Nakabayashi N. Preparation of phospholipid polymers and their properties as polymer hydrogel membranes. Polym J 1990;22:355–360.

13. Kurtz S, Mowat F, Ong K, Chan N, Lau E, Halpern M. Prevalence of primary and revision total hip and knee arthroplasty in the United States from 1990 through 2002. J Bone Joint Surg Am 2005;87:1487–1497.
14. Harris WH. The problem is osteolysis. Clin Orthop Relat Res 1995;311:46–53.
15. Sochart DH. Relationship of acetabular wear to osteolysis and loosening in total hip arthroplasty. Clin Orthop Relat Res 1999;363:135–150.
16. Oonishi H, Clarke IC, Good V, Amino H, Ueno M. Alumina hip joints characterized by run-in wear and steady-state wear to 14 million cycles in hip-simulator model. J Biomed Mater Res A 2004;70:523–532.
17. McMinn DJ, Daniel J, Pynsent PB, Pradhan C. Mini-incision resurfacing arthroplasty of hip through the posterior approach. Clin Orthop Relat Res 2005;441:91–98.
18. Muratoglu OK, Bragdon CR, O'Connor DO, Jasty M, Harris WH. A novel method of cross-linking ultra-high-molecular-weight polyethylene to improve wear, reduce oxidation, and retain mechanical properties. Recipient of the 1999 HAP Paul Award. J Arthroplasty 2001;16:149–160.
19. Moro T, Takatori Y, Ishihara K, Konno T, Takigawa Y, Matsushita T, Chung UI, Nakamura K, Kawaguchi H. Surface grafting of artificial joints with a biocompatible polymer for preventing periprosthetic osteolysis. Nat Mater 2004;3:829–837.
20. Moro T, Takatori Y, Ishihara K, Nakamura K, Kawaguchi H. 2006 Frank Stinchfield Award: Grafting of biocompatible polymer for longevity of artificial hip joints. Clin Orthop Relat Res 2006;453:58–63.
21. Kyomoto M, Moro T, Konno T, Takadama H, Yamawaki N, Kawaguchi H, Takatori Y, Nakamura K, Ishihara K. Enhanced wear resistance of modified cross-linked polyethylene by grafting with poly(2-methacryloyloxyethyl phosphorylcholine). J Biomed Mater Res A 2007;82:10–17.
22. Kyomoto M, Moro T, Konno T, Takadama H, Kawaguchi H, Takatori Y, Nakamura K, Yamawaki N, Ishihara K. Effects of photo-induced graft polymerization of 2-methacryloyloxyethyl phosphorylcholine on physical properties of cross-linked polyethylene in artificial hip joints. J Mater Sci Mater Med 2007;18:1809–1815.
23. Kyomoto M, Moro T, Miyaji F, Konno T, Hashimoto M, Kawaguchi H, Takatori Y, Nakamura K, Ishihara K. Enhanced wear resistance of orthopaedic bearing due to the cross-linking of poly(MPC) graft chains induced by γ-ray irradiation. J Biomed Mater Res B Appl Biomater 2008;84:320–327.
24. Kyomoto M, Moro T, Miyaji F, Hashimoto M, Kawaguchi H, Takatori Y, Nakamura K, Ishihara K. Effect of 2-methacryloyloxyethyl phosphorylcholine concentration on photo-induced graft polymerization of polyethylene in reducing the wear of orthopaedic bearing surface. J Biomed Mater Res A 2008;82:439–447.
25. Goda T, Konno T, Takai M, Moro T, Ishihara K. Biomimetic phosphorylcholine polymer grafting from polydimethylsiloxane surface using photo-induced polymerization. Biomaterials 2006;27:5151–5160.
26. Goda T, Konno T, Takai M, Ishihara K. Photoinduced phospholipid polymer grafting on Parylene film: Advanced lubrication and antibiofouling properties. Colloids Surf B Biointerfaces 2007;54:67–73.
27. ISO. Plastics-Film and sheeting-Measurement of water-contact angle of corona-treated films. International Organization for Standardization 15989, 2004.
28. ASTM F732-00: Standard test method for wear testing of polymeric materials used in total joint prostheses. In: Annual Book of ASTM Standards 13, 2004.
29. ISO. Implants for surgery: Wear of total hip-joint prostheses, Part 1: Loading and displacement parameters for wear-testing machines and corresponding environmental conditions for test. International Organization for Standardization 14242-1, 2002.
30. ISO. Implants for surgery: Wear of total hip-joint prostheses, Part 2: Methods of measurement. International Organization for Standardization 14242-2, 2000.
31. Kobayashi M, Terayama Y, Hosaka N, Kaido M, Suzuki A, Yamada N, Torikai N, Ishihara K, Takahara A. Friction behavior of high-density poly(2-methacryloyloxyethyl phosphorylcholine) brush in aqueous media. Soft Matter 2007;2:740–746.
32. de Vicente J, Stokes JR, Spikes HA. Soft lubrication of model hydrocolloids. Food Hydrocolloids 2006;20:483–491.
33. Matsuda T, Kaneko M, Ge S. Quasi-living surface graft polymerization with phosphorylcholine group(s) at the terminal end. Biomaterials 2003;24:4507–4515.
34. Raviv U, Frey J, Sak R, Laurat P, Tadmor R, Klein J. Properties and interactions of physigrafted end-functionalized poly (ethylene glycol) layers. Langmuir 2002;18:7482–7495.
35. Raviv U, Glasson S, Kampf N, Gohy JF, Jérôme R, Klein J. Lubrication by charged polymers. Nature 2003;425:163–165.
36. Ishikawa Y, Hiratsuka K, Sasada T. Role of water in the lubrication of hydrogel. Wear 2006;261:500–504.
37. Yamasaki A, Imamura Y, Kurita K, Iwasaki Y, Nakabayashi N, Ishihara K. Surface mobility of polymers having phosphorylcholine groups connected with various bridging units and their protein adsorption-resistance properties. Colloids Surf B Biointerfaces 2003;28:53–62.
38. Ishihara K, Nomura H, Mihara T, Kurita K, Iwasaki Y, Nakabayashi N. Why do phospholipid polymers reduce protein adsorption? J Biomed Mater Res 1998;39:323–330.
39. Hoshi T, Sawaguchi T, Konno T, Takai M, Ishihara K. Preparation of molecular dispersed polymer blend composed of polyethylene and poly(vinyl acetate) by in situ polymerization of vinyl acetate using supercritical carbon dioxide. Polymer 2007;48:1573–1580.
40. Wang A, Essner A, Polineni VK, Stark C, Dumbleton JH. Lubrication and wear of ultra-high molecular weight polyethylene in total joint replacements. Tribol Int 1998;31:17–33.
41. Tateiwa T, Clarke IC, Shirasu H, Masaoka T, Shishido T, Yamamoto K. Effect of low protein concentration lubricants in hip simulators. J Orthop Sci 2006;11:204–211.

Suppression of Protein Adsorption on a Charged Phospholipid Polymer Interface

Yan Xu,*,† Madoka Takai,* and Kazuhiko Ishihara

Department of Materials Engineering, School of Engineering, and Center for NanoBio Integration, The University of Tokyo, 7-3-1, Hongo, Bunkyo-ku, Tokyo 113-8656, Japan

Received September 9, 2008

High capability of a charged interface to suppress adsorption of both anionic and cationic proteins was reported. The interface was covalently constructed on quartz by modifying with an anionic phospholipid copolymer, poly(2-methacryloyloxyethyl phosphorylcholine (MPC)-*co*-*n*-butyl methacrylate (BMA)-*co*-potassium 3-methacryloyloxypropyl sulfonate (PMPS)-*co*-3-methacryloxypropyl trimethoxysilane (MPTMSi)) (PMBSSi). The PMBSSi interfaces were very hydrophilic and homogeneous and could function effectively for a long time even under long-term fluidic working conditions. The PMBSSi density on the interface, which was controllable by adjusting the PMBSSi concentration of the modification solution, affected the surface properties, including the surface contact angle, the surface roughness, and the surface ζ-potential. When a PMBSSi modification was applied, the adsorption of various proteins (isoelectric point varying from 1.0 to 11.0) on quartz was reduced to at least 87% in amount, despite the various electrical natures these proteins have. The protein adsorption behavior on the PMBSSi interface depended more on the PMBSSi density than on the surface charge. The PMBSSi modification had a stable impact on the surface, not only at the physiologic ionic strength, but also over a range of the ionic strength, suggesting that electrostatic interactions do not dominate the behavior of protein adsorption to the PMBSSi surface.

1. Introduction

Prevention of nonspecific protein adsorption is important in various areas, such as biological assays, medical diagnostics, drug discovery, and surgery. Methods to overcome the nonspecific protein adsorption to surfaces have been developed. One way is to physically or chemically modify the surface of the material. Various surface modification materials including polymers have been finely reviewed in literature.[1,2] Among them, one of the most attractive polymers is poly(2-methacryloyloxyethyl phosphorylcholine) (poly(MPC)) and its derivatives.[3,4] The concept behind the incorporation of phosphorylcholine(PC) moieties onto surfaces by modification with MPC polymers evolved from the fact that the zwitterionic phospholipids, which are major components of the cell membrane, have been shown to significantly resist protein adsorption. Accordingly, the MPC polymers possess excellent biological and biomedical benefits from a bulk class to micro- and nanoscales.[5−7] Especially in the novel field of microfluidic chip devices (or the so-called micrototal analysis systems (μ-TAS) and lab-on-a-chip systems), which have promised a new era of chemistry, biology, and medicine in miniaturized systems, recently we have developed several MPC polymers to modify major chip substrate materials.[8,9] For example, poly(MPC-*co*-*n*-butyl methacrylate (BMA)) (PMB), which has shown biocompatibility to human whole blood, was successfully applied to a microcapillary chip for a blood serum assay.[10] To our knowledge, this is the first time the MPC moieties have been immobilized in a microfluidic chip. In addition, poly(MPC-*co*-3-methacryloxypropyl trimethoxysilane (MPTMSi)) (PMSi), a copolymer composed of the MPC and a methacrylate with a silane coupling moiety (MPTMSi), by which we have constructed a MPC polymer covalent coating via a silanization process in a glass microchip.[11] We have demonstrated that the PMSi coating could effectively suppress both protein adsorption and cell adhesion in an electro-osmotic flow (EOF) actuated cell sorter chip. The EOF, as a state-of-the-art approach widely applied in miniaturized systems for fluid delivery, offers many advantages, features such as easy control and simple miniaturization.[12] Nevertheless, the EOF in the PMSi-coated microchannel was too weak to efficiently handle cells, because PMSi is a neutral polymer with a ζ-potential of nearly 0 mV. Other researchers have also successfully developed some neutral polymers to resist nonspecific protein adsorption in microfluidic chips, but they have the same limitation as PMSi in the EOF generation.[13]

To explore the possibility and capability of applying the MPC polymer to electrokinetically actuated microfluidic chips with biological applications, it is very necessary to further modify the polymer architecture of the recently available PMSi with incorporating the charge. Potassium 3-methacryloyloxypropyl sulfonate (PMPS), which contains an anionically charged group, was therefore first introduced for this purpose. While Lewis et al. has reported incorporation of cationic moieties within a MPC copolymer to selectively induce interactions between the coated surface and cells or other molecules,[14] to induce the EOF, anionic moieties are generally considered to be favorable. As a methacrylate monomer, PMPS not only is commercially available and well documented in literature,[15,16] but also has reactivity to the other methacrylate monomers such as MPC.[17] As described above, the structure of the modified PMSi is poly(MPC-*co*-BMA-*co*-PMPS-*co*-MPTMSi) and is referred to as PMBSSi. In a preceding paper, we detailed the synthesis and characterization of PMBSSi and emphasized on the electrokinetic properties of the PMBSSi-coated

* To whom correspondence should be addressed. Tel.: +81-3-5841-7233 (Y.X.); +81-3-5841-7125 (M.T.). Fax: +81-3-5841-6039 (Y.X.); +81-3-5841-8647 (M.T.). E-mail: xuyan@icl.t.u-tokyo.ac.jp (Y.X.); takai@mpc.t.u-tokyo.ac.jp (M.T.).

† Present address: Department of Applied Chemistry, School of Engineering, The University of Tokyo.

10.1021/bm801279y CCC: $40.75
Published on Web 12/18/2008

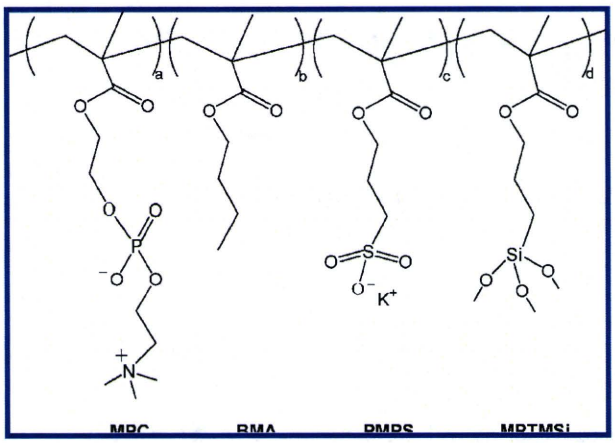

Figure 1. Chemical structure of poly(MPC-*co*-BMA-*co*-PMPS-*co*-MPTMSi) (PMBSSi).

quartz.[18] The surface ζ-potential was seen to increase with the increase of the polymer concentration for coating. Consequently, the magnitude of the EOF in the modified microchannel could be modulated by only adjusting the coating concentration. Because this control is dependent on surface differences rather than the change in the buffer composition of many conventional methods, it would be more suited to miniaturized systems for biological applications requiring neutral buffer conditions. Importantly, the study primarily revealed that the anionically charged groups of PMBSSi had no unfavorable effect on the suppression of protein adsorption. This suggests that the possibly increased electrostatic interactions from the surface charge may not dominate the protein adsorption/desorption process in the PMBSSi system. To elucidate this point, the relationships between various factors and the resistance of protein adsorption should be further investigated. These factors would include surface properties, protein properties, and buffer properties, which are generally thought as key factors involved in the process of the protein adsorption to surfaces.[19,20] Herein we, in particular, describe and discuss how these factors affect the suppression of protein adsorption when the charged MPC polymer coating is applied and thereby try to elucidate the ability of MPC to resist protein adsorption when it consists in a copolymer system with other charged moieties. This not only is certainly important for charged MPC polymers to be applied in microfluidic devices as well as other biomedical fields, but also would be meaningful for elucidating the mechanism of the protein adsorption to a charged surface.

2. Experimental Section

Synthesis of Anionic Phospholipid Copolymer. The anionic phospholipid copolymer, poly(MPC-*co*-BMA-*co*-PMPS-*co*-MPTMSi) (PMBSSi, shown in Figure 1), was synthesized according to the process described by us previously.[18] In summary, first, the desired amounts of MPC (synthesized as reported by us elsewhere),[21] BMA (Kanto Chemicals, Tokyo, Japan), PMPS (Tokyo Kasei Kogyo Co., Tokyo, Japan), MPTMSi (Kanto Chemicals), and α,α′-azobisisobutyronitrile (AIBN, Kanto Chemicals, as initiator) were dissolved in ethanol in a flask at room temperature. Then the radical polymerization was performed in the sealed flask at 60 °C for 6 h. Finally, the polymer product was reprecipitated from an ether/chloroform (7/3, v/v) mixture solvent and dried in vacuo. The structure of the copolymer was identified by ^{1}H NMR. The average molecular weight (M_w) was determined by a gel permeation chromatography (GPC) system (JASCO International Co., Ltd., Tokyo, Japan). The molecular properties of PMBSSi are listed in Table 1.

Surface Coating. Quartz substrates (Sendai Quartz and Glass, Sendai, Japan) with 0.5 mm thickness were used for coating. The PMBSSi ethanol solutions were used as coating solutions without any additives. After being cleaned by ethanol and O_2 plasma treatment, the substrate was ready for a dip-coating procedure: the cleaned substrate was first immersed in the polymer solution of the desired concentration for 2 h, then, the substrate was dried under nitrogen, and after that, the coated substrate was further dried in a vacuum condition overnight. Before being used for characterization and investigation, the samples were first rinsed by the distilled water to wash off the remained unreacted PMBSSi molecules, then dried under nitrogen, and dried again in a vacuum condition overnight.

Surface Characterization. *XPS Analysis.* The surface elemental composition was determined by X-ray photoelectron spectroscopy (XPS) (Axis-His, Shimadzu/KRATOS, Kyoto, Japan). XPS analyses were carried out under a high vacuum condition of 1×10^{-9} Torr or less. The X-ray source was Mg Kα (1253.6 eV) and the electric current was 10 mA. The takeoff angle employed was 90°. For each sample, three samples were analyzed.

Evaluation of Coating Stability. The quartz plates coated with PMBSSi were first fixed with stainless wires and then rinsed in distilled water undergoing magnetic stirring at 300 rpm. All the plates were kept under the same rinsing conditions. The plates were removed after rinsing for 1, 5, 25, and 45 h. The elemental compositions on the surfaces of the rinsed plates were analyzed by XPS. At least three samples for each rinsing duration were measured. As controls, samples without fluidic rinsing were also measured (i.e., elemental compositions at 0 h).

Coating Density Measurement. The coating density was determined with a quartz crystal microbalance (QCM). QCM has been widely used to measure the mass of material/molecules attached to the surface of the quartz crystal via changes in the resonant frequency (Δf).[22,23] The resonant frequency of the sensor crystal (f) depends on the total oscillating mass. When a thin film is attached to the sensor crystal, the frequency decreases. The resonant frequency shift of the QCM is due to the change in the total coupled mass. If the film is thin and rigid, the decrease in frequency is proportional to the mass of the film. In this way, the QCM operates as a very sensitive balance. The mass of the adhering layer is calculated by using the Sauerbrey relation[24]

$$\Delta m = -\frac{C \cdot \Delta f}{n} \tag{1}$$

where C (= 17.7 ng Hz^{-1} cm^{-2} for f = 5 MHz crystals) is the mass sensitivity constant and n (= 1, 3,...) is the overtone number. In this study, all measurements were performed using a Q-Sense D300 system (Q-Sense AB, Göteborg, Sweden). The Q-Sense software package was employed to acquire experimental data and to evaluate the data with modeling fittings. For the accurate modeling, the measuring at multiple frequencies (i.e., 5, 15, 25, and 35 MHz) was simultaneously applied. The SiO_2 coated (SiO_2/Au) sensor crystal was first cleaned by reactive oxygen plasma. Then the resonant frequency of the sensor crystal (f_c) was previously measured. Next, the active side of the sensor crystal was spin-coated with the PMBSSi solution of the desired concentration. After that, the PMBSSi coated sensor was dried in a vacuum condition overnight. To wash off the remaining unreacted PMBSSi, the coated crystal was rinsed with distilled water, dried under nitrogen, and further dried in a vacuum condition overnight. Finally, the resonant frequency of the PMBSSi coated sensor crystal (f_p) was measured. In this case, ($f_p - f_c$) is the change in the resonant frequency (Δf), by which the mass of PMBSSi per unit area (defined as *coating density*) can be calculated through the Sauerbrey relation. Because the coating process for a sensor crystal is almost the same as that for a quartz substrate, the PMBSSi coating on the sensor is considered identical with that on the quartz substrate.

Contact Angle Measurement. The static water contact angle of the surface was measured by using a CA-W automatic contact angle meter (Kyowa Interface Science, Saitama, Japan); for each sample, at least six different areas were measured and averaged.

AFM Analysis. The surface morphology was characterized by an atomic force microscopy (AFM; Bioscope, Nanoscope IIIa, Veeco,

Table 1. Molecular Properties of PMBSSi

abb.	composition (mole fraction)[a] [MPC/BMA/PMPS/MPTMSi]	molecular weight (M_w)[b]	polydispersity ratio (M_w/M_n)[c]	solubility[d] H_2O	solubility[d] EtOH
PMBSSi	46/32/9/13	1.2×10^4	1.2	+	+

[a] Determined by ^{1}H NMR. [b] Weight average molecular weight (M_w); determined by GPC, PEO standard. [c] M_n: number average molecular weight. [d] Evaluated by dissolving 0.1 g polymer powder in a 10 mL solvent; +: soluble.

Table 2. Properties and Related Information of Proteins Used in the Study

proteins[a]	approximate isoelectirc point (*pI*)	approximate molecular weight (M_w)/kDa	source
pepsin	1.0	35.0	porcine stomach mucosa
albumin	4.7	66.0	bovine serum
fibrinogen	5.5	340.0	bovine plasma
γ-globulins	5.8–7.3	150.0	bovine blood
hemoglobin	6.8–7.0	64.5	bovine blood
myoglobin	7.0/7.4	17.6	horse skeletal muscle
α-chymotrypsin	8.8	25.0	bovine pancreas
ribonuclease A	9.5	13.7	bovine pancreas
cytochrome c	10.0–10.5	12.4	horse heart
lysozyme	11.0	14.3	chicken egg white

[a] Except for myoglobin (Wako Pure Chemical Industries, Ltd., Tokyo, Japan), all the other proteins were purchased from Aldrich-Sigma (St. Louis, MO).

Santa Barbara, CA). Measurements under dry conditions were performed using the tapping mode of operation with a phosphorus (n) doped silicon cantilever (RTESP). For in situ AFM measurements in solution (1X Dulbecco's Phosphate-Buffered Saline (D-PBS), pH 7.1, Invitrogen Company, Carlsbad, CA) wet condition, a nonconductive silicon nitride cantilever (NP-S20) was used in tapping mode in the fluid. The roughness of the surface topographies (10×10 μm^2 area) was characterized by measuring the root-mean-square (rms) roughness of the AFM images.

Surface ζ-Potential Measurement. The surface ζ-potential was measured in a 10 mM NaCl solution using an electrophoretic light-scattering spectrophotometer (ELS 8000, Otsuka Electron., Osaka, Japan) with a plate cell; for every sample, the determination was repeated six times.

EOF Measurement. A method taking advantage of the migration data collected with a suitable neutral and inert tracer in an open channel under an applied electric field was applied to estimate the EOF mobility. This method has been presented elsewhere,[25] including in our previous work.[18] In this research, the measurements of the EOF behaviors were performed using the microchannel with polystyrene microspheres (Polybead) as neutral tracers, whose average diameter was 6.0 μm. 1X D-PBS (adjusted to pH 7.0) was used as a buffer in the measurements.

Investigation of Protein Adsorption. The evaluation of the protein adsorption was conducted on the quartz substrates ($20 \times 20 \times 0.5$ mm^3) with various proteins listed in Table 2. Protein solutions (0.32 g L^{-1}) prepared in 1X D-PBS buffer (pH 7.1) were used for all the experiments except for studies on ionic strength effect on the amount of adsorption, in which additional NaCl (50 and 150 mM) was spiked in the 1X D-PBS to given concentrations. The protocol for determining the amount of protein adsorption on a sample surface is described as follows. First, after the coated and uncoated (control) quartz plates were equilibrated overnight in distilled water, they were immersed in 10 mL of protein solution and incubated at 37 °C for 1 h to achieve adequate contact between the quartz plates and the protein. Then the plates were removed and rinsed in sufficient 1X D-PBS (pH 7.1), undergoing 300 rpm magnetic stirring to remove the unabsorbed protein; this rinsing procedure was conducted twice for 5 min each time. To detach all the adsorbed protein from the quartz plate, each plate was placed in a small case with 2.0 mL of 10 mg mL^{-1} sodium dodecyl sulfate (SDS) solution (water as solvent) in which the quartz plate was adequately immersed. The sealed case was treated via ultrasonication for 10 min, and the amount of protein in the SDS solution was determined by the Micro BCA protocol (Micro BCA Protein Assay Kit, Pierce Biotechnology, Rockford, IL).[26]

3. Results and Discussion

Preparation of Charged Phospholipid Copolymer Coating. Table 1 shows the molecular properties of PMBSSi. The MPTMSi moieties in the synthesized anionic phospholipid copolymer (PMBSSi) possess silanization reactivity. A silanization process is an effective way to chemically change the surface properties of silica-based substrates, because these substrates contain hydroxyl groups which attack and displace the alkoxy groups on the silane-coupling agents thus forming a covalent -Si–O–Si- bond. The silanization strategy has been widely applied in microfluidic chip devices for surface modification, because silica-based substrates such as quartz and glass are initial and popular substrate materials to fabricate and develop microfluidic devices. British workers have first reported an incorporation of silane-coupling moieties in a MPC copolymer for inducing cross-linking among polymer molecules,[27] while we have first constructed a MPC polymer interface via a silanization process in a quartz microchip by a MPC polymer composed of MPC and MPTMSi.[11] In this study, the MPTMSi moieties were also incorporated for the same purpose. After hydrolysis, the PMBSSi macromolecules attack the hydroxyl groups of the SiO_2 substrate, thus forming a covalent -Si–O–Si- bond via a dehydration process (with heat or in vacuo). In the synthesized PMBSSi, the mole fraction of the MPTMSi moieties is 13%. This composition is sufficient because, as reported in our previous research, a composition of 10% (mole fraction) MPTMSi in copolymer was sufficient to make a covalent coating on quartz.[11] In PMBSSi, the mole fraction of MPC units is 46%. This is a composition in consideration of both the suppression of the protein adsorption and the solubility of the copolymer because the MPC copolymer having more than 30% MPC units in mole fraction is apt to dissolve in water and some other representative protic solvents such as ethanol.[28] In fact, PMBSSi can be dissolved in both water and ethanol, which is favorable in surface modifications of various devices, especially microfluidic devices. Therefore, alcoholic solutions of PMBSSi were used as coating solutions without any other additives. This enables easy handling, quick treatment, and nearly no solvent remnants after treatment. The coating process is very simple, as described in Experimental Section, just a conventional dip coating, and can be quickly completed in 2 h.

XPS analysis was used to confirm the modification of the quartz surface. The binding energy (BE) scale was corrected using C_{1s} as a reference at BE = 285 eV. The six elements present in PMBSSi can be identified from their XPS peaks: silicon (Si_{2p}, BE ~ 102 eV), phosphorus (P_{2p}, BE ~ 133 eV), sulfur (S_{2p}, BE ~ 168 eV), carbon (C_{1s}, BE ~ 285 eV), nitrogen (N_{1s}, BE ~ 402 eV), and oxygen (O_{1s}, BE ~ 533 eV). The spectra of nitrogen (N_{1s}) and phosphorus (P_{2p}) at a takeoff angle of 90° were shown in Figure 2. Nitrogen (N_{1s}) and phosphorus (P_{2p}) were detected on both the high-concentration (3.00 mg mL^{-1}) and low-concentration (0.30 mg mL^{-1}) PMBSSi coated

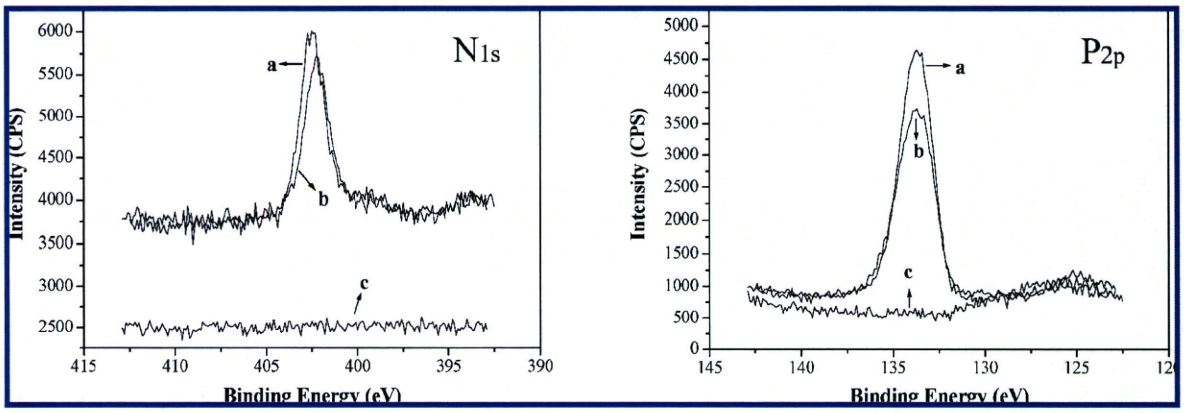

Figure 2. XPS spectra of nitrogen (N_{1s}) and phosphorus (P_{2p}) on different sample surfaces: (a) quartz surface with a high-concentration (3.00 mg mL^{-1}) PMBSSi coating (i.e., high-density coating sample); (b) quartz surface with a low-concentration (0.30 mg mL^{-1}) PMBSSi coating (i.e., low-density coating sample); (c) uncoated quartz surface (i.e., noncoating sample). The spectra were recorded using a takeoff angle of 90° with respect to the sample surface.

surfaces but not on the uncoated quartz surface, indicating the presence of MPC units on the coated surfaces and therefore the success of the surface modification. In addition, the relative peak intensities of both elements were decreased with increasing the concentration of PMBSSi, implying that comparing with the high-concentration coating, the low-concentration coating might make more amount of PMBSSi reacted on the substrate.

Surface Properties. As XPS analyses suggest, the concentration of the polymer coating solution may influence the amount of polymer coated to the quartz surface. To confirm this, we further determined the densities of coatings by a method with the QCM. The modeling with the Q-sense software program indicated that in the case of the high-concentration (3.00 mg mL^{-1}) PMBSSi coating, the resulting thickness of the coating is 87 nm, while the Sauerbrey relation resulted in 88 nm, meaning that this particular film could just be analyzed by the Sauerbrey relation. The coating surface densities of the high-concentration (3.00 mg mL^{-1}) and low-concentration (0.30 mg mL^{-1}) PMBSSi coated surfaces measured by the QCM were 11.14 ± 0.05 $\mu g\ cm^{-2}$ and 1.19 ± 0.01 $\mu g\ cm^{-2}$, respectively. This indicates that the coating density of the high-concentration (3.00 mg mL^{-1}) PMBSSi coating is almost 10 times higher than that of the low-concentration (0.30 mg mL^{-1}) PMBSSi coating, a same difference as exhibited in coating concentrations. Figure 3 demonstrates the relationship between the polymer coating concentration and the coating density. In the figure, noncoating (density = 0.00 $\mu g\ cm^{-2}$), low-density coating (density = 1.19 $\mu g\ cm^{-2}$), and high-density coating (density = 11.14 $\mu g\ cm^{-2}$) represent the uncoated, low-concentration (0.30 mg mL^{-1}) PMBSSi coated and high-concentration (3.00 mg mL^{-1}) PMBSSi coated quartz surfaces, respectively. A linear fit is applicable to describe the relationship between the coating concentration and the coating density, which reveals that the coating density can be adjusted by changing the coating concentration of the polymer solution.

The coating density affected the surface properties including the surface contact angle, the surface roughness and the surface ζ-potential. These surface properties of different samples are listed in Table 3. After the quartz surfaces were coated with PMBSSi, the water contact angle on the surface decreased from 31.2 ± 1.2 degree (noncoating) to 23.8 ± 2.8 degree in the case of the low-density coating and to 13.4 ± 1.3 degree in the case of the high-density coating. The uncoated quartz surface is hydrophilic and the decrease in the contact angle after coating indicates that the coating made the surface more hydrophilic

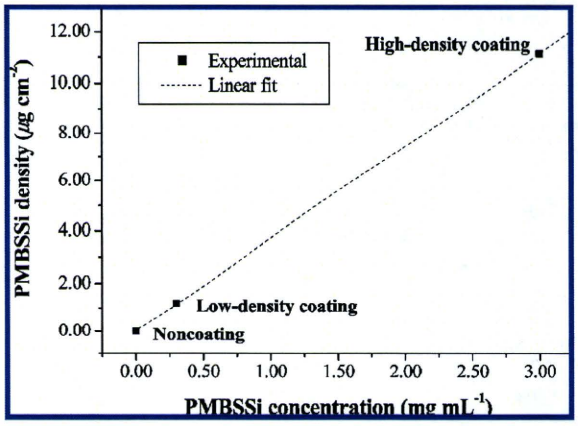

Figure 3. PMBSSi densities on sample surfaces plotted vs PMBSSi concentrations for coating. A linear fit ($y = 0.04 + 3.70x$, $R^2 = 1.00$) is applicable to describe the relationship between the PMBSSi coating density and the PMBSSi concentration for coating.

than the original surface. The rms roughness analyses of AFM observations can provide quantitative information on surface homogeneity. On the one hand, all the samples (noncoating, low-density coating, and high-density coating) exhibited quite low rms roughness values less than 0.80 nm under both dry and PBS wet conditions, indicating that these sample surfaces were homogeneous under both conditions. On the other hand, the calculated rms values also exhibited some subtle changes in roughness as a result of the coating. For example, the rms roughness in dry condition decreased from 0.51 (noncoating) to 0.30 nm (low-density coating) and 0.32 nm (high-density coating) after coating. This decrease could be attributed to the filling of the topographical structure with PMBSSi, leading to smoother surfaces. In addition, the high-density coating had almost the same rms value (0.32 nm) as that of the low-density coating (0.30 nm) in dry conditions. Under PBS wet conditions, the PMBSSi coatings changed the topologies of the surfaces, increasing the roughness values, yielding rms values of 0.79 and 0.69 nm for the low-density coating and the high-density coating, respectively. This increase would be due to the stretching and swelling of the PMBSSi chains in PBS. Surface charge conditions were characterized with the surface ζ-potential. As determined, the quartz surface is negatively charged with a ζ-potential of -47.4 ± 0.9 mV. After coating with PMBSSi, the surface ζ-potential changed, because charged moieties (PMPS moieties) on PMBSSi in place of hydroxyl

Table 3. Surface Properties of Different Sample Surfaces

sample	density[a] (μg cm^{-2})	contact angle[b] (°)	rms roughness (nm) dry	rms roughness (nm) wet	ζ-potential[c] (mV)
noncoating	0.00	31.2 ± 1.2	0.51	0.60	−47.4 ± 0.9
low-density coating	1.19 ± 0.01	23.8 ± 2.8	0.30	0.79	−14.3 ± 1.9
high-density coating	11.14 ± 0.05	13.4 ± 1.3	0.32	0.69	−24.2 ± 2.5

[a] Data are mean ± SD, $n = 3$. [b] Data are mean ± SD, $n \geq 6$. [c] Data are mean ± SD, $n = 6$.

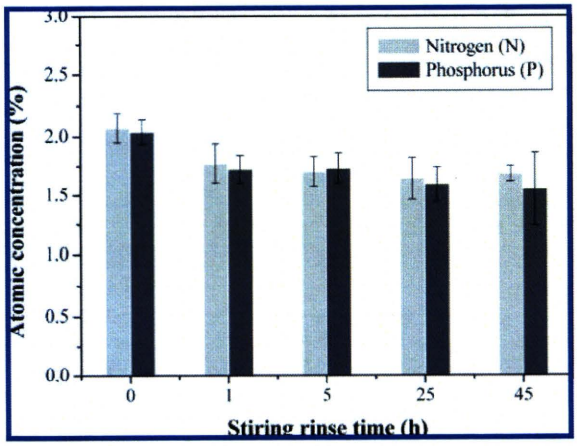

Figure 4. Change in atomic concentration of nitrogen and phosphorus (determined by XPS) on the quartz surfaces with the high-density PMBSSi coatings before (0 h) and after rinsing by stirring at 300 rpm in distilled water for 45 h. Data are mean ± SD, $n = 3$.

groups on the original quartz surface became to dominate the charge condition of the outmost surface. Table 3 indicates that, the low-density coating exhibited a lower (absolute value of) surface ζ-potential (−14.3 ± 1.9 mV) than the high-density coating (−24.2 ± 2.5 mV), owing to the lower amount of PMPS moieties on the low-density coating than on the high-density coating. The coating density further influenced the electrokinetic property of the surface by altering the surface ζ-potential. The EOF determination indicated that the PMBSSi-coated quartz surface retained a significant amount of cathodic EOF.[18] For example, in the condition of 1X D-PBS (adjusted to pH 7.0), the EOF mobility of a quartz microchannel with the high-density PMBSSi coating was $(0.99 \pm 0.14) \times 10^{-4}$ cm^2 V^{-1} s^{-1}, which is roughly more than half (53%) that of the uncoated microchannel under the same buffer conditions.

The evaluation of the coating stability provided evidence that the PMBSSi coating is a type of stable coating. The investigations were carried out in distilled water undergoing a quite high speed of magnetic stirring (300-rpm). As demonstrated in Figure 4, the surface atomic concentrations of nitrogen (N) and phosphorus (P) on the quartz surfaces with high-density PMBSSi coatings, which were determined by XPS, remained at almost the same levels during the entire long-term (45 h) rinse process. Therefore, the PMBSSi coating layer could not be detached by the fluidic rinse. This reveals that the PMBSSi coating can function effectively for a long time even under long-term fluidic working conditions.

Suppressing Protein Adsorption by Coating. To investigate the ability of the charged polymer coating to suppress protein adsorption, various proteins with different isoelectric points (*pI*), a critical pH point at which a protein carries no net electrical charge, were employed to quantitatively evaluate protein adsorptions on coated quartz surfaces. The information of these proteins is listed in Table 2. All the samples were analyzed by the MicroBCA protein analysis protocol, which is usually applied to determine protein amounts in solutions with very low protein concentrations.[26] In the same batch, uncoated quartz surfaces were also analyzed as controls. All the protein solutions were prepared in 1X D-PBS (pH 7.1), which is a physiological buffer condition that is conventionally applied in many biological analyses. The results are arranged based on the *pI* values of the proteins in order to elucidate the effects of the charge conditions of the PMBSSi coatings on protein adsorption. The results are shown in Figure 5. All proteins, both the anionic and cationic ones, had high adsorption amounts on the uncoated quartz surfaces, and in contrast, had significantly low adsorption amounts on the PMBSSi coated surfaces. For example, bovine serum albumin (BSA, $pI = 4.7$, anionic) and lysozyme (LYZ, $pI = 11.0$, cationic) had adsorption amounts of 1.47 μg cm^{-2} and 0.35 μg cm^{-2}, respectively, on the uncoated surfaces (noncoating); but these amounts are reduced to 0.17 μg cm^{-2} and 0.02 μg cm^{-2}, respectively, on the surfaces with high-density PMBSSi coatings. When a high-density coating was applied, the amount reduction in adsorption was at least 87% and, in some cases (for example, α-chymotrypsin), was more than 99%. That is to say, proteins, both anionic and cationic ones, hardly adsorb onto the surfaces constructed by PMBSSi, although it is charged.

Effect of Coating Density. The protein adsorption to a surface depends on the surface properties to some extent. As described previously, the differences in surface properties of PMBSSi coating can be essentially attributed to the difference in surface coating density. Hence, it is useful to obtain a relationship between the coating density and the amount of protein adsorbed on the charged surface. Comparing the data of the amounts of adsorbed protein (Figure 5), we found that after coating with PMBSSi, both the high-density coating and the low-density coating caused a dramatic decrease in the protein adsorption. There was, however, some slight difference in the amounts of protein adsorption between the two cases. All the protein adsorption data indicated that the surface with the high-density coating exhibited much lower amounts of protein adsorption than the surface with the low-density coating. For example, taking pepsin ($pI = 1.0$, anionic) and ribonuclease A ($pI = 9.5$, cationic) as instances, in the case of pepsin, the amounts adsorbed on the low- and high-density coatings were 0.55 μg cm^{-2} and 0.18 μg cm^{-2}, respectively, and in the case of ribonuclease A, they were 0.29 μg cm^{-2} and 0.08 μg cm^{-2}, respectively. That is, the amounts of adsorbed protein in both cases deceased with increasing the PMBSSi coating density. The same tendencies in the effect of the coating density were obtained in all the cases of the other proteins. As aforementioned (Table 3), an increase in the PMBSSi density resulted in an increase in the absolute value of the surface ζ-potential. In some conventional surfaces, as the absolute value of the surface ζ-potential increases, the electrostatic interactions between the surface and the protein would increase, and therefore the risk of protein adsorption would also increase.[20] However, in the PMBSSi coated surfaces, the increase in the surface ζ-potential resulted from the increase in the PMBSSi density, did not lead to more amounts of protein adsorbed to the surfaces, and

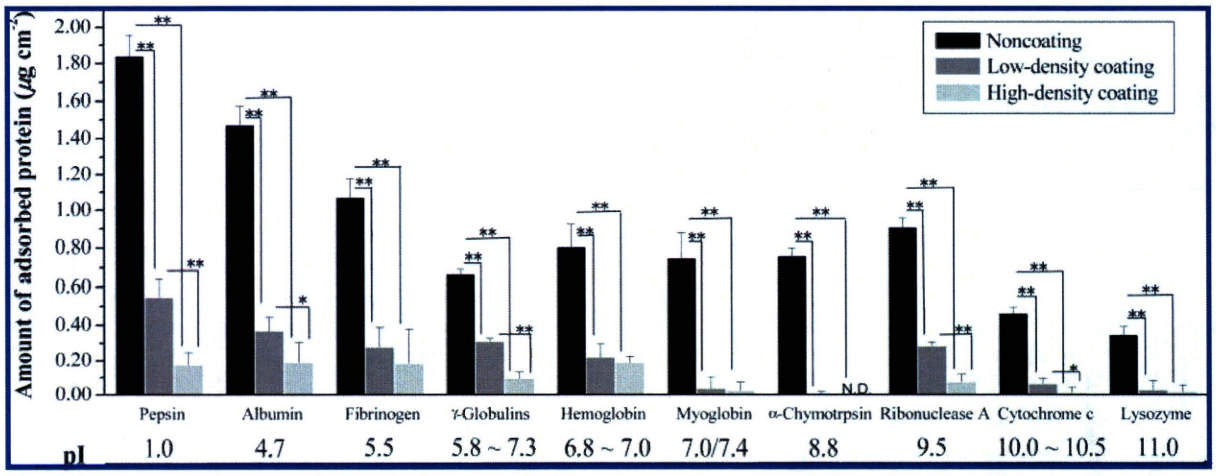

Figure 5. Amounts of various proteins with *pI* values varying from 1.0 to 11.0 absorbed on different sample surfaces. Data are mean ± SD, $n = 9$. Statistical difference significance: *, $p < 0.01$; **, $p < 0.001$.

contrarily, made more reduction in the amount of protein adsorption. This suggests that the PMBSSi density should be the key factor which affects the protein adsorption/resistance on the PMBSSi coated surface. It is known that the PC groups of MPC units play a key role in the suppression of protein adsorption in the MPC polymer coating. More PC groups mean a higher capability to suppress the protein adsorption to some extent. Comparing with the low-density coating, the high-density coating made more PMBSSi react with the quartz surface and thereby afforded a higher composition of MPC units (or PC groups) in the coating layer. This contributed to more reduction in protein adsorption in the high-density coating. In addition, comparing with the high-density coating, the low-density coating has a looser steric structure of coating layer, which may create more chances for some proteins to penetrate into the inner layer of the coating and, consequently, lead to an increase in the amount of protein adsorption. Therefore, in the PMBSSi coating system, we consider that the amount of proteins in the PMBSSi surface might depend more on the PMBSSi density than on the surface charge of the coating.

Effect of Buffer Ionic Strength. The ionic strength of a buffer is generally considered to remarkably affect a protein adsorbing from buffer to a charged surface because counterion concentration affects the degree to which the surface charge is shielded. To further elucidate the role of surface charge in the protein adsorption to PMBSSi coated surfaces, the adsorption behaviors were studied in buffers with different ionic strengths. The increase of the ionic strength was obtained by addition of NaCl to 1X D-PBS. Both BSA and LYZ adsorptions were studied as functions of the addition of NaCl. As shown in Figures 6 and 7, the amounts of BSA and LYZ adsorbed on the uncoated quartz surfaces (noncoating) decreased dramatically with the addition of NaCl in the range of 0 mM to 150 mM. This can be explained by the screened electrostatic interactions occurring at high ionic strength. This reveals that the uncoated quartz surface was intensely sensitive to the electrostatic conditions. However, in contrast to the adsorption behavior on the uncoated quartz surface, which displayed strong ionic strength sensitivity, the BSA adsorption on both the low- and the high-density coated quartz surfaces were not significantly affected by the increase in the ionic strength (Figure 6). The similar behavior also exhibited in the LYZ adsorption, which is shown in Figure 7. These profiles indicate that the PMBSSi coating has an impact on the surface, not only at the physiologic ionic strength but also over a range of the ionic strength.

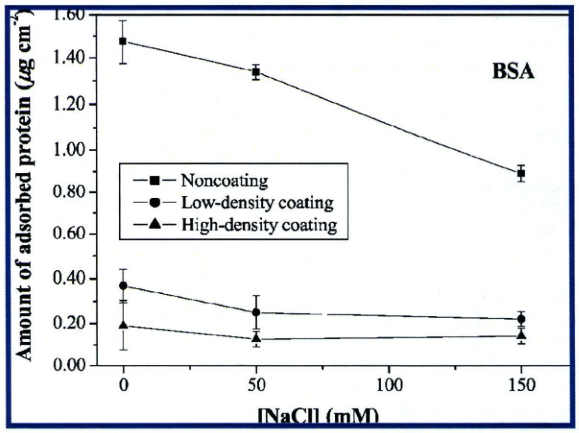

Figure 6. Influence of the buffer ionic strength on the amount of bovine serum albumin (BSA, *pI* = 4.7, anionic) adsorbed on different sample surfaces. The increase of the buffer ionic strength was obtained by addition of NaCl to 1X D-PBS (pH 7.1). [NaCl] represents the added NaCl concentration and the NaCl concentration of original 1X D-PBS (about 137 mM) is not included. Data are mean ± SD, $n = 9$.

Moreover, the buffer ionic strength has no pronounced influence on protein adsorption to the PMBSSi modified surface, suggesting that this process was not dominated by electrostatic interactions between protein molecules and the surface.

Although the understanding of the mechanism and the physics of protein resistance specific to MPC-based surface remains in complete in the present time, several hypotheses or theories have been proposed based on common understandings and our group's research.[4,29,30] The research let us be aware of the importance of exploring water interactions among the surface and around the environment to understand the protein resistance. If the water state at the surface is similar to an aqueous solution, protein does not need to release bound water molecules even if protein molecules contact the surface. This means that the hydrophobic interaction does not occur between proteins and the polymer surface. Moreover, the conformational change in the protein's three-dimensional structure during protein adsorption on or contact with the surface does not happen. Our research elucidated that MPC-based polymers usually carry higher level of free water fraction on the polymer surface, as is well-known that PC groups are highly hydrated. Thus, proteins can contact the surface reversibly, without significant conformational change.

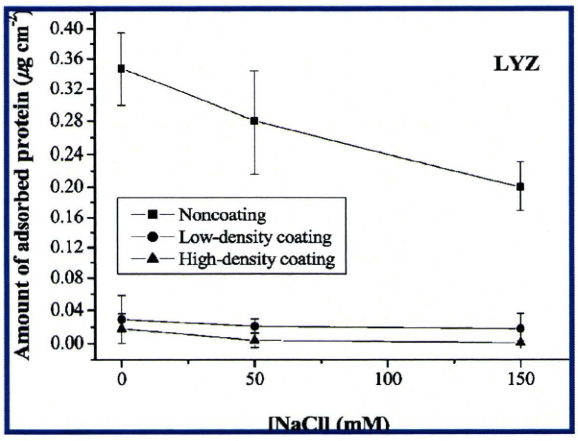

Figure 7. Influence of the buffer ionic strength on the amount of lysozyme (LYZ, *pI* = 11.0, cationic) adsorbed on different sample surfaces. The increase of the buffer ionic strength was obtained by addition of NaCl to 1X D-PBS (pH 7.1). [NaCl] represents the added NaCl concentration and NaCl concentration of original 1X D-PBS (about 137 mM) is not included. Data are mean ± SD, $n = 9$.

The results of the simulation work suggested that PC head groups are very quickly surrounded and polarized by the water molecules when contacting with water.[31] Further, Kitano et al. found that the structure of the aqueous solution surrounded PC groups is very close to that of pure water by the Raman spectrum.[32]

As charged units (PMPS) involved, however, PMBSSi is more complicated than other noncharged MPC polymers. In this work, the experimental results suggest that the amount of surface charge was shown to be a poor determinant of protein adsorption (Figure 5). Accordingly, the effect of electrostatic interactions on the adsorption of the proteins studied is minimal or neglectable (Figures 6 and 7). This tests and supports the hypothesis proposed by Lewis, A. L. that, even though the surface charge of the MPC polymer coating is changed by incorporation of the monomer having charged groups, if a significant proportion of PC in the composition exists, the interaction of the protein with the charged surface may still be similar to that with a surface of a noncharged MPC polymer coating.[33] This group demonstrated adding cationic charge to MPC polymer with the cationically charged monomer choline methacrylate (CMA), that all polymer coatings containing 0—23% CMA (mole fraction, converted from the weight percentage originally described by the authors in the reference) exhibited small amounts of protein adsorption, with no statistical difference.[33] In the PMBSSi, the mole fraction of MPC monomers is 46%, which is predominant among all components. In contrast, the anionically charged monomer PMPS is only 9% in mole fraction, an amount that is considered incapable of inducing significant amounts of protein adsorption. In addition, in the case of the PMBSSi coating, the increase of the buffer ionic strength by addition of NaCl does not remarkably change the property of the PC dominated interface, so it does not significantly affect the resistance of protein adsorption on the surface. Therefore, the charge in the PMBSSi not only satisfies the requirement for generation of the electrokinetic phenomena but also has no adverse effect on suppression of the protein adsorption.

4. Conclusions

We described a charged interface constructed on the silica-based substrate with a charged phospholipid copolymer (PMBSSi) coating with the covalent bonding, which has high capability to suppress adsorption of both anionic and cationic proteins. The PMBSSi interfaces were very hydrophilic and homogeneous, and could function effectively for a long time even under long-term fluidic working conditions. The coating density, which was controllable by adjusting the polymer coating concentration, affected the surface properties including the surface contact angle, the surface roughness and the surface ζ-potential. When a PMBSSi coating was applied, the adsorption of various proteins with a wide range of *pI* (1.0−11.0) on quartz was suppressed significantly to at least 87% in amount. The high-density coating, though exhibited a higher surface ζ-potential, showed much higher reduction in the amount of protein adsorption in comparison with the low-density coating, indicating that the protein adsorption behavior on the PMBSSi interface depends more on the surface density than on the surface charge. This was explained by the fact that the higher density coating affords more composition of PC groups on the interface when on contact with water. Further, in contrast to the adsorption behavior on the uncoated quartz surface, which displayed strong ionic strength sensitivity, protein adsorption on PMBSSi coated quartz surfaces were not remarkably affected by the change in the ionic strength. That is, the PMBSSi coating has an impact on the surface, not only at the physiologic ionic strength but also over a range of the ionic strength, revealing that electrostatic interactions do not dominate the behavior of protein adsorption to the PMBSSi surface. Therefore, the PMBSSi interface holds the capability to be applied to electrokinetically actuated microfluidic chips with biological applications, for not only suppressing the unfavorable protein adsorption but also simultaneously generating favorable electrokinetic phenomena.

Acknowledgment. This study was supported in part by Scientific Research(B) 16310084 from Grants-in-Aid for Scientific Research of Japan Society for the Promotion of Science (JSPS) and by Asahi Glass Foundation (2004).

References and Notes

(1) Werner, C.; Maitz, M. F.; Sperling, C. *J. Mater. Chem.* **2007**, *17*, 3376–3384.
(2) Jordan, S. W.; Chaikof, E. L. *J. Vasc. Surg.* **2007**, *45*, 104A–115A.
(3) Iwasaki, Y.; Ishihara, K. *Anal. Bioanal. Chem.* **2005**, *381*, 534–546.
(4) Ishihara, K.; Nomura, H.; Mihara, T.; Kurita, K.; Iwasaki, Y.; Nakabayashi, N. *J. Biomed. Mater. Res.* **1998**, *39*, 323–330.
(5) Feng, W.; Zhu, S. P.; Ishihara, K.; Brash, J. L. *Biointerphases* **2006**, *1*, 50–60.
(6) Kaji, H.; Kawashima, T.; Nishizawa, M. *Langmuir* **2006**, *22*, 10784–10787.
(7) Goto, Y.; Matsuno, R.; Konno, T.; Takai, M.; Ishihara, K. *Biomacromolecules* **2008**, *9*, 828–833.
(8) Sakai-Kato, K.; Kato, M.; Ishihara, K.; Toyo'oka, T. *Lab Chip* **2004**, *4*, 4–6.
(9) Sibarani, J.; Takai, M.; Ishihara, K. *Colloid Surf., B* **2007**, *54*, 88–93.
(10) Oki, A.; Adachi, S.; Takamura, Y.; Ishihara, K.; Ogawa, H.; Ito, Y.; Ichiki, T.; Horiike, Y. *Electrophoresis* **2001**, *22*, 341–347.
(11) Takai, M.; Onoda, H.; Ishihara, K.; Takamura, Y.; Horiike, Y. In *Micro Total Analysis Systems 2004*, Laurell, T., Nilsson, J., Jensen, K., Harrison, D. J., Eds.; Royal Soc. Chem.: Cambridge, U.K., 2005; Vol. 2, pp 115−117.
(12) Stone, H. A.; Stroock, A. D.; Ajdari, A. *Annu. Rev. Fluid Mech.* **2004**, *36*, 381–411.
(13) Wu, D. P.; Zhao, B. X.; Dai, Z. P.; Qin, J. H.; Lin, B. C. *Lab Chip* **2006**, *6*, 942–947.
(14) Lewis, A. L.; Berwick, J.; Davies, M. C.; Roberts, C. J.; Wang, J. H.; Small, S.; Dunn, A.; O'Byrne, V.; Redman, R. P.; Jones, S. A. *Biomaterials* **2004**, *25*, 3099–3108.
(15) Masci, G.; Bontempo, D.; Tiso, N.; Diociaiuti, M.; Mannina, L.; Capitani, D.; Crescenzi, V. *Macromolecules* **2004**, *37*, 4464–4473.
(16) Roland-Swanson, C.; Besse, J. P.; Leroux, F. *Chem. Mater.* **2004**, *16*, 5512–5517.

(17) Ito, T.; Iwasaki, Y.; Narita, T.; Akiyoshi, K.; Ishihara, K. *Colloid Surf., B* **2005**, *41*, 175–180.
(18) Xu, Y.; Takai, M.; Konno, T.; Ishihara, K. *Lab Chip* **2007**, *7*, 199–206.
(19) Glomm, W. R.; Halskau, O.; Hanneseth, A. M. D.; Volden, S. *J. Phys. Chem. B* **2007**, *111*, 14329–14345.
(20) Pasche, S.; Voros, J.; Griesser, H. J.; Spencer, N. D.; Textor, M. *J. Phys. Chem. B* **2005**, *109*, 17545–17552.
(21) Ishihara, K.; Ueda, T.; Nakabayashi, N. *Polym. J.* **1990**, *22*, 355–360.
(22) Marx, K. A. *Biomacromolecules* **2003**, *4*, 1099–1120.
(23) Andersson, M.; Andersson, J.; Sellborn, A.; Berglin, M.; Nilsson, B.; Elwing, H. *Biosens. Bioelectron.* **2005**, *21*, 79–86.
(24) Sauerbray, G. Z. *Phys.* **1959**, *155*, 206–222.
(25) Rathore, A. S. *Electrophoresis* **2002**, *23*, 3827–3846.
(26) Pierce Biotechnology, Inc. Pierce 2003−2004 Applications Handbook and Catalog; Pierce Biotechnology, Inc.: Rockford, IL, 2003, pp 241−243.
(27) Lewis, A. L.; Cumming, Z. L.; Goreish, H. H.; Kirkwood, L. C.; Tolhurst, L. A.; Stratford, P. W. *Biomaterials* **2001**, *22*, 99–111.
(28) Konno, T.; Watanabe, J.; Ishihara, K. *J. Biomed. Mater. Res., Part A* **2003**, *65*, 209–214.
(29) Ishihara, K.; Oshida, H.; Endo, Y.; Ueda, T.; Watanabe, A.; Nakabayashi, N. *J. Biomed. Mater. Res.* **1992**, *26*, 1543–1552.
(30) Morisaku, T.; Watanabe, J.; Konno, T.; Takai, M.; Ishihara, K. *Polymer* **2008**, *49*, 4652–4657.
(31) Sheng, Q.; Schulten, K.; Pidgeon, C. *J. Phys. Chem.* **1995**, *99*, 11018–11027.
(32) Kitano, H.; Imai, M.; Mori, T.; Gemmei-Ide, M.; Yokoyama, Y.; Ishihara, K. *Langmuir* **2003**, *19*, 10260–10266.
(33) Palmer, R. R.; Lewis, A. L.; Kirkwood, L. C.; Rose, S. F.; Lloyd, A. W.; Vick, T. A.; Stratford, P. W. *Biomaterials* **2004**, *25*, 4785–4796.

BM801279Y

New in 2009 ACS APPLIED MATERIALS & INTERFACES

Letter

Self-Initiated Surface Graft Polymerization of 2-Methacryloyloxyethyl Phosphorylcholine on Poly(ether ether ketone) by Photoirradiation

Masayuki Kyomoto, and Kazuhiko Ishihara

ACS Appl. Mater. Interfaces, **2009**, 1 (3), 537-542• DOI: 10.1021/am800260t • Publication Date (Web): 16 February 2009

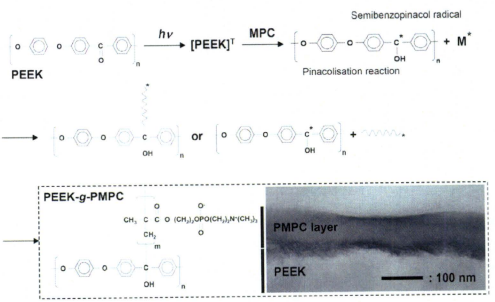

More About This Article

Additional resources and features associated with this article are available within the HTML version:

- Supporting Information
- Access to high resolution figures
- Links to articles and content related to this article
- Copyright permission to reproduce figures and/or text from this article

View the Full Text HTML

LETTER

Self-Initiated Surface Graft Polymerization of 2-Methacryloyloxyethyl Phosphorylcholine on Poly(ether ether ketone) by Photoirradiation

Masayuki Kyomoto[*,†,‡,§] **and Kazuhiko Ishihara**[‡,||]

Research Department, Japan Medical Materials Corporation, 3-3-31 Miyahara, Yodogawa-ku, Osaka 532-0003, Japan, and Department of Materials Engineering, School of Engineering, Division of Science for Joint Reconstruction, School of Medicine, and Center for NanoBio Integration, The University of Tokyo, 7-3-1 Hongo, Bunkyo-ku, Tokyo 113-8656, Japan

ABSTRACT In the present paper, we reported the fabrication of a highly hydrophilic nanometer-scale modified surface on a poly(ether ether ketone) (PEEK) substrate by photoinduced graft polymerization of 2-methacryloyloxyethyl phosphorylcholine (MPC) in the absence of photoinitiators. Photoirradiation results in the generation of semibenzopinacol-containing radicals of benzophenone units in the PEEK molecular structure, which acts as a photoinitiator during graft polymerization. The poly(MPC)-grafted PEEK surface fabricated by a novel and simple polymerization system exhibited unique characteristics such as high wettability and high antiprotein adsorption, which makes it highly suitable for medical applications.

KEYWORDS: poly(ether ether ketone) • phosphorylcholine • surface modification • photopolymerization • wettability • protein adsorption

INTRODUCTION

Poly(aryl ether ketone) (PAEK), including poly(ether ether ketone) (PEEK), is a relatively new family of high-temperature thermoplastic polymers, consisting of an aromatic backbone molecular chain interconnected by ketone and ether functional groups; i.e., a benzophenone (BP) unit is included in its molecular structure. Polyaromatic ketones exhibit enhanced mechanical properties, and their chemical structure is stable at high temperatures, resistant to chemical and radiation damages, and compatible with many reinforcing agents (such as glass and carbon fibers); therefore, they are considered to be promising materials for industrial applications such as aircraft, turbine blades, and electric devices. In the 1990s, the biocompatibility and in vivo stability of various PAEK materials and high-performance engineering polymers were investigated (1). Recently, PEEK has emerged as the leading high-performance thermoplastic candidate for replacing metal implant components, especially in the field of orthopedics and trauma (2). In recent studies, the tribological and bioactive properties of PEEK, which is used as a bearing material and flexible implant in joint arthroplasty, have been investigated (3–5). However, conventional single-component PEEK cannot satisfy these requirements (e.g., wear resistance or fixation with a bone) for the artificial joint (2). Because of interest in further improving implants, the PEEK as biomaterials study has also been focused on the biocompatibility of the polymer, either as a reinforcing agent or as a surface modification (6, 7). Therefore, multicomponent polymer systems have been designed in order to synthesize new multifunctional biomaterials. In order to use PEEK and related composites in novel implant applications, they can be engineered to have a wide range of physical, mechanical, and surface properties.

2-Methacryloyloxyethyl phosphorylcholine (MPC), a methacrylate monomer composed of a phospholipid polar group, which is identical with the neutral phospholipids of cell membranes, is used to synthesize polymer biomaterials having excellent biocompatibility (8–12). MPC polymers, exhibiting a cell membrane like structure, have potential application in various fields such as biology, biomedical science, and surface chemistry because they exhibit several unique properties such as good biocompatibility, high lubricity, low friction, and excellent antiprotein adsorption (8–12).

Surface modification is one of the most important technologies for the preparation of new multifunctional biomaterials. In general, a polymer surface can be modified using the following two methods: (a) surface absorption or reaction with small molecules and (b) grafting of polymeric molecules onto a substrate via a covalent bond. Grafting polymerization is performed most frequently using either of the following methods: (i) surface-initiated graft polymerization termed the "grafting from" method in which the monomers are polymerized from initiators or comonomers and (ii) adsorption of the polymer to the substrate termed the "grafting to"

* Tel: +81-6-6350-1014. Fax: +81-6-6350-5752. E-mail: kyomotom@jmmc.jp.
Received for review December 22, 2008 and accepted February 5, 2009
† Japan Medical Materials Corp.
‡ Department of Materials Engineering, School of Engineering, The University of Tokyo.
§ Division of Science for Joint Reconstruction, School of Medicine, The University of Tokyo.
|| Center for NanoBio Integration, The University of Tokyo. E-mail: ishihara@mpc.t.u-tokyo.ac.jp.
DOI: 10.1021/am800260t

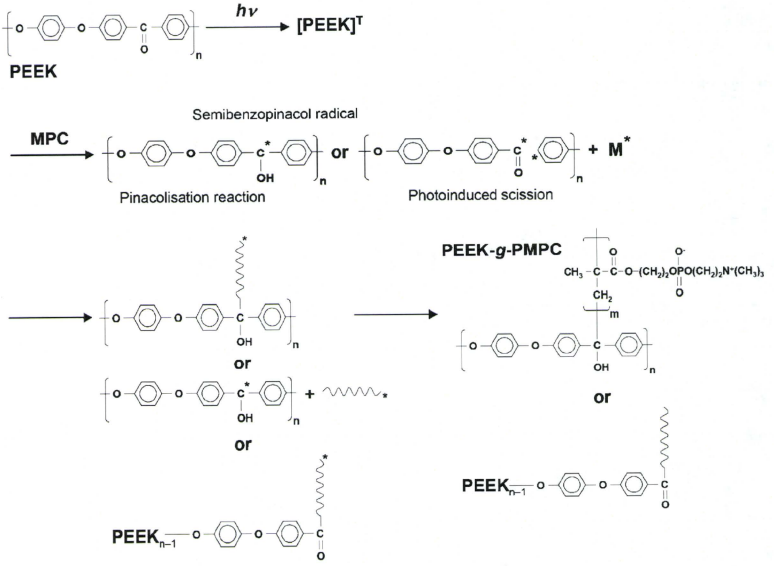

FIGURE 1. Scheme for the preparation of PEEK-*g*-PMPC.

methods such as dipping, cross-linking, or reaction of the end groups of the ready-made polymers with the functional groups of the substrate. The "grafting from" method has an advantage over the "grafting to" method in that it forms a high-density polymer brush interface with a multifunctional polymer; this advantage results in a fruitful function. In previous studies, a multifunctional biomaterial such as poly(MPC) (PMPC) was grafted onto a polyethylene (PE) surface; this was accomplished using photoinduced "grafting from" polymerization in the presence of a conventional BP photoinitiator (13−17). During grafting, the physically adsorbed BP initiators on the PE surface were excited to the triplet-state hydrogen (H) atom from the $-CH_2-$ group of the PE surface; this resulted in the formation of radicals that were capable of inducing surface-initiated graft polymerization, which was conducted under ultraviolet (UV) irradiation.

In this study, we have demonstrated the fabrication of a biocompatible and highly hydrophilic nanometer-scale modified surface by grafting PMPC onto the surface of a self-initiated PEEK using a novel photoinduced "grafting from" polymerization reaction. We hypothesize that photoirradiation results in the generation of semibenzopinacol-containing radicals of the BP units in PEEK, which acts as a photoinitiator during the "grafting from" polymerization. It is well-known that when BP is exposed to photoirradiation such as UV irradiation, a pinacolization reaction is induced; this results in the formation of semibenzopinacol (ketyl) radicals that act as photoinitiators. Our technique enables the direct grafting of PMPC onto the PEEK surface in the absence of a photoinitiator, thereby resulting in the formation of a C−C covalent bond between the PMPC and PEEK substrate. The chemical and physical properties of the PEEK surface were also investigated.

MATERIALS AND METHODS

PMPC Graft Polymerization. The preparation of PMPC-grafted PEEK (PEEK-*g*-PMPC) is schematically illustrated in Figure 1. PEEK specimens were machined from an extruded PEEK (450G; Victrex plc, Thornton-Cleveleys, U.K.) bar stock, which was fabricated without stabilizers and additives. The surfaces of the PEEK specimens were ultrasonically cleaned in ethanol for 20 min and then dried in vacuum. MPC was industrially synthesized using the method reported by Ishihara et al. (8) and supplied by the NOF Corp. (Tokyo, Japan). It was dissolved in degassed water to obtain a 0.5 mol/L aqueous solution; PEEK specimens were immersed in this solution. Photoinduced graft polymerization was carried out at 60 °C for 90 min on the PEEK surface under UV irradiation (UVL-400HA ultrahigh-pressure mercury lamp; Riko-Kagaku Sangyo Co., Ltd., Funabashi, Japan) with an intensity of 5 mW/cm^2; a filter (model D-35; Toshiba Corp., Tokyo, Japan) was used to restrict the passage of UV light to wavelengths of 350 ± 50 nm. After polymerization, the PEEK-*g*-PMPC specimens were removed from the MPC solution, washed with pure water and ethanol to remove nonreacted monomers and nongrafted polymers, and dried at room temperature. As a reference sample, a PEEK-*g*-PMPC with BP was prepared by PMPC grafting with BP precoating. Before PMPC grafting, the PEEK specimens were immersed in an acetone solution containing 10 mg/mL of BP (Wako Pure Chemical Industries, Ltd., Osaka, Japan) for 30 s and then dried in the dark at room temperature in order to remove the acetone. It was reported that the amount of BP adsorbed on the surface was 3.5×10^{-11} mol/cm^2 (9).

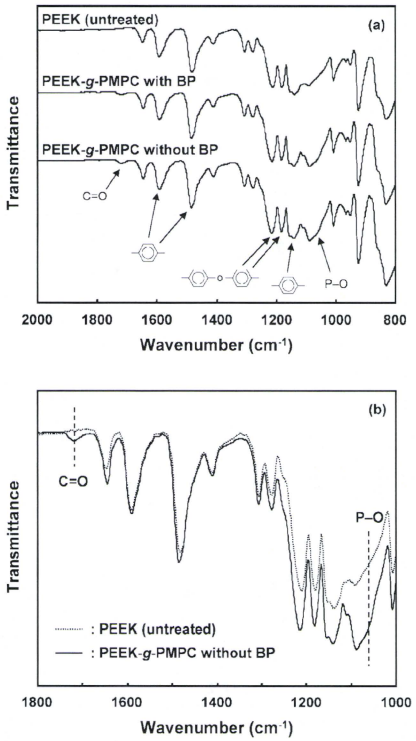

FIGURE 2. FT-IR/ATR spectra of PEEK-*g*-PMPC with/without BP.

Surface Analysis by Fourier Transform Infrared (FT-IR) Spectroscopy, X-ray Photoelectron Spectroscopy (XPS), and Water-Contact Angle Measurement. The functional group vibrations of the PEEK-*g*-PMPC surface that was grafted with/without BP were examined using attenuated total reflection (ATR) by FT-IR spectroscopy. FT-IR/ATR spectra were obtained in 32 scans over a range of 800−2000 cm^{-1} at a resolution of 4.0 cm^{-1} by using an FT-IR analyzer (FT/IR615; Jasco International Co., Ltd., Tokyo, Japan).

The surface elemental contents of the PEEK-*g*-PMPC surface that was grafted with/without BP were analyzed using XPS. XPS spectra were obtained using an XPS spectrophotometer (AXIS Hsi 165; Kratos/Shimadzu Corp., Kyoto, Japan) equipped with a Mg Kα radiation source by applying a voltage of 15 kV at the anode. The takeoff angle of the photoelectrons was maintained at 90°. Each measurement was scanned five times, and five replicate measurements were performed on each sample; their average values were considered for determining the surface elemental contents.

The static water-contact angles of the PEEK-*g*-PMPC surface that was grafted with/without BP were measured with an optical bench-type contact angle goniometer (model DM300; Kyowa Interface Science Co., Ltd., Saitama, Japan) using a sessile drop method. Drops of purified water (1 μL) were deposited on the PEEK-*g*-PMPC surface, and the contact angles were measured directly after 60 s by using a microscope. Subsequently, 15 replicate measurements were performed on each sample, and the average values were taken as the contact angles.

Cross-Sectional Observation of PEEK-*g*-PMPC Using Transmission Electron Microscopy (TEM). The cross section of the PMPC layer fabricated on the PEEK-*g*-PMPC surface that was grafted with/without BP was observed using a transmission electron microscope. First the specimens were embedded in an epoxy resin, stained with a ruthenium oxide vapor at room temperature, and then sliced into ultrathin films (approximately 100 nm thick) using a Leica Ultracut UC microtome (Leica Microsystems, Ltd., Wetzlar, Germany). A JEM-1010 electron microscope (JEOL, Ltd., Tokyo, Japan) was used for TEM observation at an acceleration voltage of 100 kV.

Characterization of Protein Adsorption by a Micro-bicinchoninic Acid (BCA) Method. The amount of protein adsorbed on the untreated PEEK and PMPC layer of the PEEK-*g*-PMPC surface that was grafted with/without BP was measured using the micro-BCA method. Each specimen was immersed in Dulbecco's phosphate-buffered saline (PBS; pH 7.4, ion strength = 0.15 M; Immuno-Biological Laboratories Co., Ltd., Takasaki, Japan) for 1 h to equilibrate the surface modified by the MPC polymer. The specimens were immersed in a bovine serum albumin (BSA; molecular weight = 6.7×10^4; Sigma-Aldrich Corp., MO) solution at 37 °C for 1 h. The protein solution was prepared in a BSA concentration of 4.5 g/L, i.e., 10% of the concentration of human plasma levels. Then, the specimens were rinsed five times with fresh PBS and immersed in a 1 mass % sodium dodecyl sulfate (SDS) aqueous solution and shaken at room temperature for 1 h to completely detach the adsorbed BSA from the PEEK surface. A protein analysis kit (micro-BCA protein assay kit, no. 23235; Thermo Fisher Scientific Inc., IL) based on the BCA method was used to determine the BSA concentration in the SDS solution, and the amount of BSA adsorbed on the PEEK surface was calculated.

Statistical Analysis. The results derived from each measurement were used to determine the water-contact angle, and the amounts of BSA adsorbed were expressed as mean values and standard deviation. The statistical significance ($p < 0.05$) was estimated by the Student's *t* test.

RESULTS AND DISCUSSION

In this study, we investigated the PMPC layer formed on the PEEK surface by photoinduced radical graft polymerization in the absence a photoinitiator. The following methods were employed in our study: (a) grafting from polymerization for the formation of a high-density graft polymer layer, (b) photoinduced polymerization in the absence of photoinitiators, and (c) use of biocompatible hydrophilic macromolecules, which exhibited photoreduction by hydrogen abstraction of a BP unit in PEEK from a hydrogen donor; this induced surface-initiated graft polymerization of the methacrylate-type monomer (i.e., MPC) on the PEEK surface, even in the absence of BP as a photoinitiator. These results are discussed hereafter.

The preparation of the PEEK-*g*-PMPC without BP is schematically illustrated in Figure 1. The present graft polymerization reaction involving free radicals is photoinduced by UV irradiation. Under UV irradiation, a BP unit in PEEK can undergo the following reactions in the aqueous MPC solutions (18−24). The pinacolization reaction (photoreduction by hydrogen abstraction of a BP unit in PEEK) results in the formation of a semibenzopinacol radical (i.e., ketyl radical),

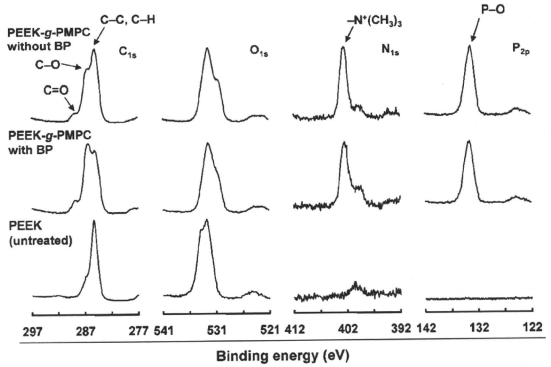

FIGURE 3. XPS spectra of PEEK-*g*-PMPC with/without BP.

Table 1. Surface Elemental Composition ($n = 5$), Static-Water Contact Angle ($n = 15$), and the Amount of BSA Adsorbed ($n = 10$) on PEEK-*g*-PMPC with/without BP

	surface elemental composition (atom %)					
sample	C_{1s}	O_{1s}	N_{1s}	P_{2p}	contact angle (deg)	amount of adsorbed BSA ($\mu g/cm^2$)
PEEK (untreated)	83.2 (0.5)[a]	16.7 (0.5)	0.1 (0.1)	0.0 (0.0)	92.5 (1.9)	0.42 (0.22)
PEEK-*g*-PMPC with BP	64.5 (1.1)	25.2 (0.8)	5.1 (0.2)	5.2 (0.2)	7.1 (1.1)	0.08 (0.08)
PEEK-*g*-PMPC without BP	62.5 (0.6)	27.3 (0.5)	5.1 (0.1)	5.1 (0.1)	6.8 (1.7)	0.08 (0.10)
PMPC[b]	57.9	31.6	5.3	5.3		

[a] The standard deviation is in parentheses. [b] Theoretical elemental composition of PMPC.

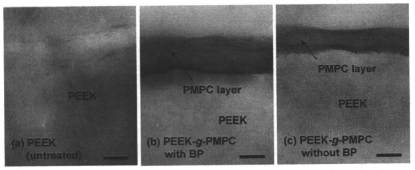

FIGURE 4. Cross-sectional TEM images of PEEK-*g*-PMPC with/without BP. Bar: 100 nm.

which can initiate the "grafting from" polymerization of MPC as the main reaction and the "grafting to" polymerization of MPC (the radical chain end of PMPC couples the semibenzopinacol radical of the PEEK surface) as a subreaction. In addition, a photoscission reaction occurs as a subreaction, which may not need a hydrogen donor. The cleavage reaction induces recombination and the "grafting from" polymerization. When water polymerization is carried out in the presence of a hydrogen donor, a phenol unit may be subsequentially formed due to hydrogen abstraction.

Figure 2 shows the FT-IR/ATR spectra of untreated PEEK and PEEK-*g*-PMPC with/without BP. Absorption peaks were observed at 1600, 1490, 1280, 1190, and 1160 cm^{-1} for both untreated PEEK and PEEK-*g*-PMPC. These peaks are chiefly attributed to the diphenyl ether group, phenyl rings, or aromatic hydrogen atoms in the PEEK substrate (25, 26). However, transmission absorption peaks at 1720 and 1080 cm^{-1} (shoulder peak) were observed only for PEEK-*g*-PMPC (Figure 2b). These peaks corresponded to the carbonyl group (C═O) and the phosphate group (P—O) in the MPC unit (15—17). The FT-IR/ATR spectra showed no clear difference between PEEK-*g*-PMPC with and without BP.

The XPS spectra of the binding energy region of the nitrogen (N) and phosphorus (P) electrons showed peaks for PEEK and PEEK-*g*-PMPC with/without BP, whereas peaks were not observed in the case of untreated PEEK (Figure 3). The peaks at 403 and 134 eV were attributed to the $-N^+(CH_3)_3$ and phosphate groups, respectively. These peaks indicate the presence of phosphorylcholine in the MPC units. After PMPC grafting, the peaks attributed to the MPC unit were clearly observed in both FT-IR/ATR and XPS spectra of PEEK-*g*-PMPC with/without BP. These peaks indicate that PMPC is successfully grafted on the surface of PEEK (15—17).

Table 1 summarizes the surface elemental compositions of the untreated PEEK and PEEK-*g*-PMPC with/without BP. The elemental compositions of N and P in all of PEEK-*g*-PMPC with/without BP were 5.2 and 5.3 atom %, respectively. The elemental composition of the PEEK-*g*-PMPC surface was almost equal to the theoretical elemental composition (atom %; N, 5.3; P, 5.3) of PMPC. These results indicate that the PMPC layer formed on the PEEK substrate covers fully.

Figure 4 shows the cross-sectional TEM images of the untreated PEEK and PEEK-*g*-PMPC with/without BP. In the